Atmospheric CO2 exchange of a small mountain lake: limitations of eddy covariance and boundary layer modeling methods in complex terrain.

Katharina Scholz[1], Elisabet Ejarque[2], Albin Hammerle[1], Martin Johann Kainz[3], Jakob Schelker[4], and Georg Wohlfahrt[1]

[1]University of Innsbruck
[2]WasserCluster Lunz - Biologische Station
[3]WasserCluster Lunz
[4]University of Vienna

November 24, 2022

Abstract

As lakes receive and transform significant amounts of terrestrial carbon, they often act as source of atmospheric CO_2. Yet, long-term measurements of lake-atmosphere CO_2 exchange with high temporal resolution are sparse. In this study, we measured the CO_2 exchange of a small lake situated in complex mountainous topography in the Austrian Alps continuously for one year. We used the eddy covariance (EC) and the boundary layer model (BLM) approaches to estimate the lake's CO_2 source or sink strength and to analyze differences between these methods.

Overall, CO_2 fluxes were small and EC measurements indicated influence of low-frequency contributions. Results from both the EC and the BLM methods indicated the lake to be a small source of atmospheric CO_2 with highest emissions in fall.

During night-time, the CO_2 concentration gradient at the air-water interface decreased due to an increase in atmospheric CO_2 above the lake, likely caused by cold and CO_2-rich air draining from the surrounding land. Consequently, BLM fluxes were lower during night-time than during daytime. This diel pattern was lacking in the EC flux measurements because the EC instruments deployed at the shore of the lake did not capture low nocturnal lake CO_2 fluxes due to the local wind regime.

Overall, this study exemplifies the relevance of the surrounding landscape for lake-atmosphere flux measurements. We conclude that estimating CO_2 evasion from lakes situated in complex topography needs to explicitly account for biases in EC flux measurements caused by low-frequency contributions and local wind systems.

Atmospheric CO_2 exchange of a small mountain lake: limitations of eddy covariance and boundary layer modeling methods in complex terrain.

K. Scholz[1], E. Ejarque[2], A. Hammerle[1], M. Kainz[2], J. Schelker[2,3], G. Wohlfahrt[1]

[1]Department of Ecology, University of Innsbruck, Sternwartestrasse 15, 6020 Innsbruck, Austria.

[2]WasserCluster Lunz – Biologische Station, Dr. Carl Kupelwieser Promenade 5, 3293 Lunz am See, Austria.

[3]Department of Functional and Evolutionary Ecology, University of Vienna, Althanstrasse 14, 1090 Vienna, Austria.

Corresponding author: Katharina Scholz (katharina.scholz@student.uibk.ac.at)

Key points:

- We estimated the CO_2 exchange of a small mountain lake using the eddy covariance and the boundary layer model approaches
- CO_2 fluxes were small and variable and the variation in local atmospheric CO_2 concentration was an important driver of lake CO_2 exchange
- The study demonstrates that the influence of the surrounding land has to be considered in lake-atmosphere flux measurements

Abstract

As lakes receive and transform significant amounts of terrestrial carbon, they often act as source of atmospheric CO_2. Yet, long-term measurements of lake-atmosphere CO_2 exchange with high temporal resolution are sparse. In this study, we measured the CO_2 exchange of a small lake situated in complex mountainous topography in the Austrian Alps continuously for one year. We used the eddy covariance (EC) and the boundary layer model (BLM) approaches to estimate the lake's CO_2 source or sink strength and to analyze differences between these methods.

Overall, CO_2 fluxes were small and EC measurements indicated influence of low-frequency contributions. Results from both the EC and the BLM methods indicated the lake to be a small source of atmospheric CO_2 with highest emissions in fall.

During night-time, the CO_2 concentration gradient at the air-water interface decreased due to an increase in atmospheric CO_2 above the lake, likely caused by cold and CO_2-rich air draining from the surrounding land. Consequently, BLM fluxes were lower during night-time than during daytime. This diel pattern was lacking in the EC flux measurements because the EC instruments deployed at the shore of the lake did not capture low nocturnal lake CO_2 fluxes due to the local wind regime.

Overall, this study exemplifies the relevance of the surrounding landscape for lake-atmosphere flux measurements. We conclude that estimating CO_2 evasion from lakes situated in complex topography needs to explicitly account for biases in EC flux measurements caused by low-frequency contributions and local wind systems.

Plain language summary

Lakes and rivers are an important link in the global carbon cycle transporting carbon from the land to the oceans. However, part of the carbon entering the water is also stored in lake sediments or released from the water into the air as carbon dioxide (CO_2). Therefore, lakes are considered important sources of atmospheric CO_2, yet long-term direct measurements of this water-air CO_2 exchange are sparse. In this study, we used two different methods to measure the CO_2 exchange of a small lake in the Austrian Alps for an entire year. We found that during the ice covered period, spring, and summer the CO_2 exchange between lake and air was small. Only in fall, the lake released CO_2 at higher rates. Overall, the lake was only a small source of CO_2 at most. We also found differences in the results of the two measuring methods. Those results demonstrated that measurements of lake-atmosphere CO_2 exchange are complex and – especially if the lake is small and situated in a mountainous landscape – the surrounding land can influence the measurements.

1. Introduction

The world's streams, rivers and lakes contribute substantially to the global carbon cycle through the emission of carbon dioxide (CO_2) across the air-water interface. Current estimates quantified that 1−3.8 Pg of carbon (C) per year are released by inland waters to the atmosphere (Aufdenkampe et al., 2011; Battin et al., 2009; Cole et al., 2007; Drake et al., 2018; Raymond et al., 2013; Tranvik et al., 2009). These CO_2 emissions are on the same order of magnitude as terrestrial net ecosystem production and net CO_2 emissions related to anthropogenic land use changes. Lakes and reservoirs account for approximately 0.3–0.64 Pg C (Aufdenkampe et al., 2011; Cole et al., 2007; Holgerson and Raymond, 2016; Raymond et al., 2013; Tranvik et al., 2009) of the total inland water CO_2 emissions, making lakes important contributors to the C balance of the earth's land surface.

Terrestrial CO_2 exchange is primarily driven by photosynthesis and respiration: atmospheric CO_2 is taken up by means of photosynthesis and stored in organic compounds in biomass. Part of this C is released back into the atmosphere through autotrophic and heterotrophic respiration and abiotic oxidation. Some terrestrial C is also exported from the land into inland waters and potentially into the ocean (Ciais et al., 2013; Drake et al., 2018). Work from the past two decades has established that inland waters not only transport terrestrial C to the coastal oceans as 'passive pipes', but are also able to process or transform C (Cole et al., 2007; Prairie and Cole, 2009). This research has concluded that only about one third to one half of the terrestrially-derived C in headwaters eventually enters the ocean. The remainder is stored in sediments or outgassed to the atmosphere (Ciais et al., 2013; Mendonça et al., 2017; Raymond et al., 2013).

The CO_2 exchange across the air-water interface is driven by the CO_2 concentration difference (ΔCO_2) between water and air and the exchange coefficient (Liss and Slater, 1974). Methods to quantify CO_2 exchange at the air-water interface include (i) concentration-gradient based methods including surface renewal or boundary layer models (BLM), (ii) chamber methods, and (iii) the eddy covariance (EC) approach.

The BLM method is based on measurements of dissolved surface water and atmospheric gas concentrations and estimates of the gas transfer velocity (k). This approach is commonly used for global estimates because reports on dissolved CO_2 concentrations are numerous and for lakes k can be modelled based on wind speed. Surface water concentrations can be measured directly using headspace equilibration methods (Bastviken et al., 2015; Cole et al., 1994; Crawford et al., 2015) or calculated from pH, alkalinity, and temperature (Libes, 2009) – quantities measured routinely at many sites (Cole et al., 1994; Hartmann et al., 2014). However, lakes from different regions are not represented equally in current datasets (Cole et al., 2007; Hartmann et al., 2014; Raymond et al., 2013) and especially data from the Alpine region are sparse (Ejarque et al., 2021; Pighini et al., 2018). Moreover, measurements are rarely done at time intervals and with adequate frequency to capture the temporal (seasonal, but also potentially diel) variability of air-water gas exchange (Zscheischler et al., 2017). Furthermore, the explicit determination of k is challenging and associated with large uncertainties. Values for k can be determined from trace gas experiments (Wanninkhof et al., 1985) or from flux measurements using for example chamber or EC methods (e.g. Jonsson et al., 2008; Vachon et al., 2010). Those methods are labor intensive or have other drawbacks and effort was put into establishing empirical relationships from existing measurements of k. To date, several models exist (Klaus and Vachon, 2020). Gas transfer is dependent on surface water turbulence which in many lakes is predominantly regulated by wind speed (Jähne et al., 1987; Read et al., 2012). Therefore, and because wind speed is quite simple to measure, wind speed is often used for determination of k. Existing studies agree on that parametrizing k as a function of wind speed is reasonable, but they also indicate that other factors like wind fetch, wave height, convection or buoyancy flux affect k (MacIntyre et al., 2010; Read et al., 2012; Vachon and Prairie, 2013) and that the wind-k-relationship might also, for example, depend on lake size and shape and therefore be lake specific (Klaus and Vachon, 2020).

With chamber methods, a fixed control volume of air is confined above the water surface by a floating chamber. By measuring the gas concentration within this volume over a defined time interval, the rate of change can be determined and used to calculate the flux across the air-water interface (e.g. Bastviken et al., 2004). Moreover, by full chamber equilibration, the water pCO_2 concentration and k can be quantified (Bastviken et al., 2015; Vingiani et al., 2020). This method is labor intensive, especially if non-automated systems are used, and covers only a small surface area. In addition, the chamber itself might influence gas exchange due to alterations of the gas concentration in the enclosure, self-heating, wind sheltering effects, and alterations of the flow field (Lorke et al., 2015; Matthews et al., 2003; Vingiani et al., 2020).

In contrast to the BLM approach, the eddy covariance (EC) method provides a tool to measure fluxes such as CO_2 exchange across a surface directly (Aubinet et al., 2012; Baldocchi et al., 1988). In principle, turbulent vertical transport of a scalar is calculated by correlating its concentration fluctuations with the vertical component of wind speed, requiring instruments with high precision and a fast response time (around 0.1 s or below). The advantages are that automated, continuous measurements are realized easily with little disturbance of the system and they are representative for a comparatively large surface area. The upwind area contributing to the measured signal is called the footprint. The footprint extends usually several hundred meters and depends on the measurement height, but also on additional factors like wind speed, surface roughness, and atmospheric stability. Requirements to acquire defensible flux measurements include that the terrain within the footprint is reasonably flat and homogenous – a condition seemingly well fulfilled for a lake surface. Although the EC method is well established for flux measurements in terrestrial environments, few long-term studies which measure gas exchange over aquatic ecosystems exist (Baldocchi, 2014; Pastorello et al., 2020). Several studies have indicated that the sharp contrast between a water surface and its surrounding land can impair the measurements. For example, different magnitudes and even direction of CO_2 fluxes on land versus water can lead to local concentration differences enhancing the potential for advective flows leading to non-turbulent/low-frequency contributions to the measured flux (Sun et al., 1998). Abrupt changes in surface roughness at the shore may influence wind speed and direction or turbulence patterns (Kenny et al., 2017).

Differences in surface characteristics (albedo, heat capacity, moisture) can lead to differential heating which in turn also drives air movement and can lead to advective air flow and the development of typical wind systems (Bischoff-Gauß et al., 2006). Because only the upwind area contributes to the EC signal, the source area depends on the wind direction. Therefore, wind patterns with typical diel variations often observed above complex terrain, like for example land and lake breezes or valley wind systems, can lead to biased results.

Although lakes are estimated to be significant emitters of CO_2, net fluxes on hourly time scales are often small and low-frequency contributions can be relatively large. Therefore, lake EC flux estimates have to follow stringent quality checks and sophisticated data processing. Sievers et al. (2015a) developed a flux analysis method that allows to determine the turbulent flux to or from a surface from EC data while separating out low-frequency influence based on ogive analysis. Application of the method in complex Arctic environments (polygonal tundra, sea ice) showed that it is advantageous for flux estimates in low flux, heterogeneous environments (Pirk et al., 2017; Sievers et al., 2015b) and therefore might also be suitable for lake flux estimates.

Here, the BLM method and the EC method in conjunction with ogive analysis were used to estimate the air-water CO_2 exchange of Lake Lunz, a small (0.68 km^2) lake situated in complex mountainous topography in the Austrian Alps, continuously for an entire year. The goal of this study was twofold: First, we aimed to compare the BLM and EC methods and to quantify and analyze differences between both methods, especially in the context of the measurement setting on a small lake in complex mountainous topography. Second, we strived to quantify the CO_2 source or sink strength of Lake Lunz and the drivers of its temporal variability in order to improve our understanding of freshwater C cycling in mountain lakes of the northern European Alps, an area which is experiencing rapid changes in climate and the hydrosphere (Blöschl et al., 2019; Gobiet et al., 2014).

We captured the temporal variation of CO_2 fluxes and related them to temporal patterns of atmospheric and aquatic CO_2 concentrations, prevailing climatic conditions, and weather events. In addition, we measured wind speed and direction at two locations on opposing shores of the lake. This allowed us to observe the local wind regime and to assess its influence on the lake and the related CO_2 exchange.

2. Material and methods

2.1. Site description

This study was performed at Lake Lunz, a clear-water oligotrophic mountain lake located in Lower Austria (47° 51′ N, 15° 03′ E), during a one year period (01.01.2017 – 31.12.2017). Lake bathymetry is steep with a mean and maximum depth of 20 m and 34 m, respectively. The lake has an oval shaped surface area of about 0.68 km^2 with its longest distance of about 1.5 km roughly aligned from west to east (Figure 1).

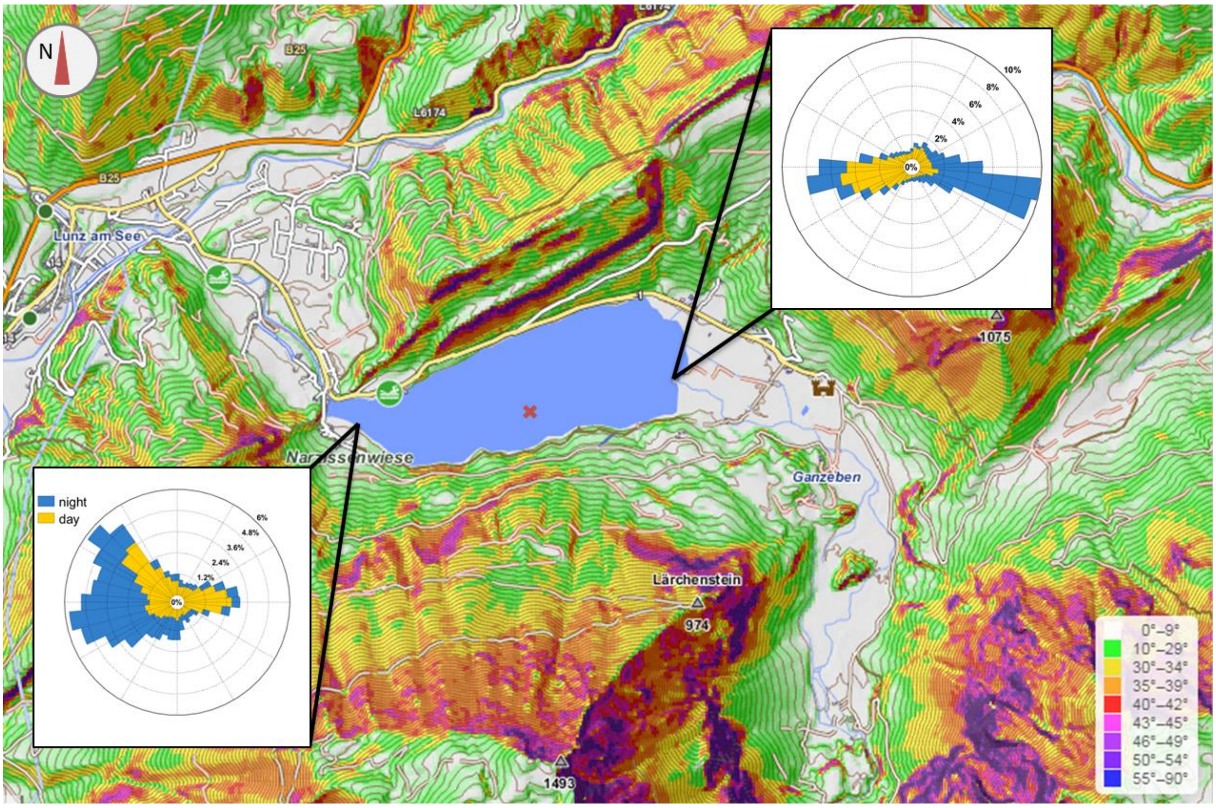

Figure 1 Topographic map of Lake Lunz and its surroundings. Inserted are the wind roses at the two measurement locations showing the frequency of day (yellow) and night-time (blue) wind directions. The red cross marks the location of the floating platform where water temperature and CO_2 concentrations were measured from spring to fall. Map from OpenSlopeMap.org.

The lake is situated in a steep and narrow valley at an elevation of 608 m.a.s.l. The ridge north of the lake reaches an elevation of about 900 m, while the slope south of the lake plateaus at about

1500 m. The north and south slopes are densely forested with spruce (*Picea abies*) and larch (*Larix decidua*). On the east side, the main lake inlet (Oberer Seebach) enters the lake and the terrain is less steep and less densely vegetated. The lake discharges into one single outlet (Unterer Seebach) at the northwest end.

2.2. Eddy covariance measurements

During 2017, EC measurements were done at the east shore on a boardwalk extending about 15 m into the lake. Previously, fluxes were measured using the same EC instruments but installed on a floating platform (Ejarque et al., 2021). However, the floating platform was only operational during summer. Moreover, the movement of the platform may influence data quality and lead to higher data rejection during quality control. Therefore, a year-round operation of EC measurements on the shore was chosen and previous wind measurements suggested highest data coverage on the east shore of the lake. The EC instruments included a 3-D sonic anemometer (R3, Gill Instruments, Lymington, UK) to measure sonic temperature and the three orthogonal wind components. CO_2 and H_2O dry mole fractions were measured using an enclosed-path infrared gas analyzer (IRGA) (LI-7200, LI-COR Inc., Lincoln, NE, USA) with a heated intake tube of 0.71 m length. Instruments were installed at 3.9 m above the lake surface (about 1.2 m from water surface to boardwalk + 2.7 m on boardwalk) and data were collected at 20 Hz. CO_2 fluxes (F_C) were calculated using the numerical ogive optimization (OgO) method (Sievers et al., 2015a). The convention that negative fluxes are towards the surface (i.e., lake as sink) and positive away from the surface (i.e., lake as source) was adopted. Only data passing the quality criteria (see below) and wind directions between 230° and 310° (wind from the lake) were considered. Measurements affected by instrument malfunctioning and data measured directly during rain events were excluded. Overall, data coverage was about 15 %.

2.2.1. Ogive flux analysis

To estimate CO_2 fluxes, we followed the OgO method (see Text S1 for additional details) developed by Sievers et al. (2015a) using the publicly available matlab toolbox OOT version 1.1.0 (Sievers, 2019);

calculations were done in Matlab version R2019b (The MathWorks Inc., Natick, MA, USA). Fluxes were calculated every 30 min. Averaging intervals were varied from 10 to 60 min around the query time. Basic quality control and preprocessing of raw data included de-spiking, gap detection, double rotation, and a time lag detection and correction (Aubinet et al., 2012; Vickers and Mahrt, 1997). Furthermore, only periods when the momentum flux in the energy containing frequency range was negative (i.e., directed towards the surface) were considered (Foken and Wichura, 1996; Sievers et al., 2015a).

2.3. Additional measurements of weather, radiation, and lake parameters

Meteorological conditions including air temperature (T_a) and relative humidity (RH), incoming and outgoing shortwave and longwave radiation (SW_{in}, SW_{out}, LW_{in}, and LW_{out}) were measured at the boardwalk. Precipitation was recorded at a nearby weather station (TAWES Lunz am See). Wind speed and wind direction were (in addition to wind measurements at the EC station on the east shore) measured at the west shore of the lake using a 3-D sonic anemometer (CSAT3, Campbell Scientific, Logan, UT, USA). From May 12th to October 18th, water temperature (T_w) profiles were measured using 9 temperature probes (CS108 and CS109SS, Campbell Scientific, Logan, UT, USA) at 0.05, 0.2, 1, 2, 4, 7, 12, 17, and 22 m below the water surface fixed to a floating platform above the deepest point of the lake (Figure 1). Meteorological data and water temperature were measured at one-minute intervals and half-hourly mean values were stored on a data logger (CR10X, Campbell Scientific, Logan, UT, USA).

On the platform, automatic measurements of atmospheric CO_2 partial pressure (pCO_{2a}) and of air equilibrated with the surface water (from ~0.3 m depth) (pCO_{2w}) were conducted from April 14th till October 29th at a three-hour interval (45 min equilibration time).

Additionally, water level was obtained from the Hydrographic Service of Lower Austria available at https://www.noel.gv.at/wasserstand/#/de/Messstellen.

2.4. Gas transfer velocity and the boundary layer model approach

We used CO_2 fluxes from the OgO analysis ($F_{C\text{-}Og}$) and measurements of atmospheric and aquatic CO_2 concentrations to determine the gas transfer velocity k and to establish the lake-specific wind speed-k relationship. This relationship was then used to extrapolate k also to times when no measurements of $F_{C\text{-}Og}$ were present. First, k was estimated as:

$$k = \frac{F_{C\text{-}Og}}{C_w - C_a} \qquad (1)$$

where C_w is the gas (e.g., CO_2) concentration in the surface water and C_a is the theoretical concentration of the gas in equilibrium with the atmosphere at the interface.

The dissolved CO_2 concentrations C_w and C_a were calculated by multiplying pCO_2 of the lake and the atmosphere, respectively, with the Henry's solubility constant H_c (equation 2 and 3):

$C_w = pCO_{2w} * H_c$ and $C_a = pCO_{2a} * H_c$; with (2)

$\ln H_c = -58.0931 + 90.5069 * \frac{100}{T_w} + 22.294 * ln\left(\frac{T_w}{100}\right)$; T_w in °K, H_c in mol L^{-1} atm^{-1}; (Weiss, 1974).

(3)

Using the Schmidt number (Sc) for CO_2 at the measured water temperature (equation 3), k was transformed to k_{600} [cm h^{-1}], the standardized gas transfer velocity at 20°C (with Sc = 600):

$$k_{600} = k * \left(\frac{600}{Sc}\right)^n \qquad (4)$$

where n = -2/3 for u < 2 m s^{-1} and n = -1/2 for higher wind speeds (Jähne et al., 1987) and

$Sc = 1911.1 - 118.11*T_w + 3.4527*T_w^2 - 0.041320 *T_w^3$; T_w in °C; (Wanninkhof, 1992). (5)

To make our results comparable to existing wind-based models, k_{600} was related to wind speed at 10 m height (U_{10}). To obtain U_{10}, sonic wind speed measured at height z_m = 3.9 m was extrapolated to 10 m height using the logarithmic wind law (equation 6):

$$U_{10} = u * ln\left(\frac{10}{z_0}\right) * \left(ln\left(\frac{z_m}{z_0}\right)\right)^{-1} \quad (6)$$

where z_0 represents the surface roughness length, which was set to 0.0001 m (Vihma and Savijärvi, 1991).

Finally, data were median-binned into 1 m s^{-1} wind classes and a linear model was fitted to k_{600} vs U_{10} (Jonsson et al., 2008). Since very small fluxes are difficult to measure and associated with large scatter, data was only considered when $C_w/C_a > 1.2$. The resulting linear model was then used to extrapolate k values (k_{600}modeled) to times when no measurements of $F_{C\text{-}Og}$ were present. By applying equation 4, k_{600}modeled was transformed to $k_{modeled}$ and the CO_2 flux $F_{C\text{-}BLM}$ was calculated based on equation 1 as:

$$F_{C\text{-}BLM} = k_{modeled} * (C_w - C_a) \quad (7)$$

Thus, and in contrast to our lake EC measurements, the calculated $F_{C\text{-}BLM}$ is independent of wind direction.

All analyses were done in Matlab version R2019b (The MathWorks Inc., Natick, MA, USA).

3. Results

3.1. Environmental conditions during the study period

Air temperature showed a typical seasonal course with high temperatures during summer and low, sometimes freezing, temperatures in winter (minimum of -20 °C in January) (Figure 2a). The mean annual temperature for 2017 at the nearby weather station was 7.7 °C, which is slightly higher than the long-term (last 20 years) mean of 7.3 °C. The maximum air temperature of 35 °C was reached at the beginning of August. Water temperature profiles were measured from May to October. During this time, the upper part of the water column (epilimnion) largely followed the seasonal course of the air temperature. The sensors down to a depth of 12 m recorded a general increase in temperature over the course of the summer, while the bottom temperature (17 m and below) stayed relatively constant around 5 °C (Figure 2a). Lake Lunz is dimictic, yet complete mixing as indicated by a uniform temperature profile around 4 °C occurred before and after our measurements started and ended in spring and fall, respectively.

Several temporary cooling periods were observed throughout the summer. The most pronounced events occurred at the end of July and in the beginning of September following large rain episodes. The air temperature reached its maximum shortly after the event in July. Also the surface water temperature increased again after the cooling event, although not reaching the previous values. The surface water temperature maximum (24.4 °C) was recorded around mid-July. After the temperature drop at the beginning of September, surface water temperatures did not recover substantially but stayed at values around 15 °C. At the same time, an increase in water temperature at 12 m depth was recorded, indicating an initial mixing of the water column to at least this depth (Figure 2a).

Annual precipitation amounted to 1725 mm. January and June were the driest months with 74 and 82 mm, respectively. This was directly reflected in the lake water level, which stayed below the long-term mean throughout those months (Figure 2b). Heavy rain events caused sharp increases in water level, most notably in winter and early spring (February and March) when they likely coincided with snowmelt (Ejarque et al., 2021), at the end of July after a long relatively dry period, and two heavy rain events in September. Rain episodes were generally associated with lower air temperature, which together with likely more groundwater inflow led to a temperature decrease in the epilimnion. In the beginning of September, almost 100 mm of rain fell within 3 days and led to a significant decrease in water temperature as described above.

The lake was covered with ice from January 1st till February 22nd (Figure 2d, blue shaded area). Until the end of the year, no new ice cover was established.

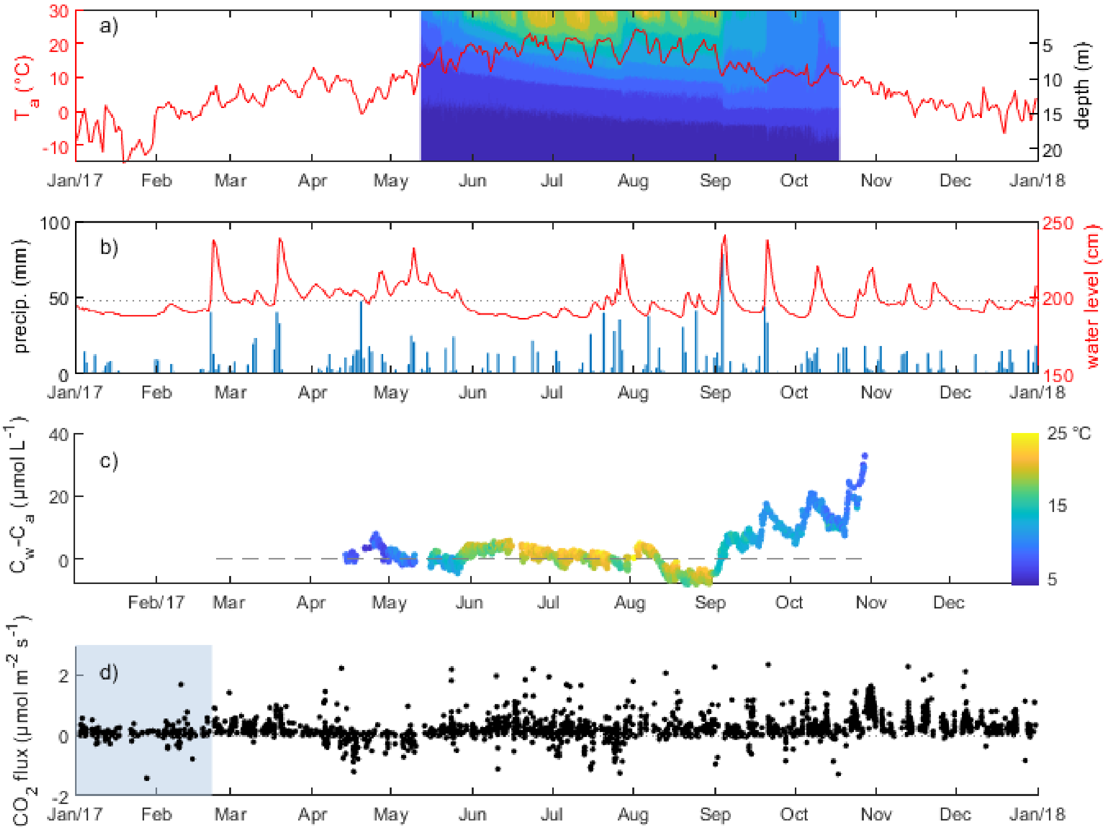

Figure 2 Seasonal course of a) Air temperature (red line) and water temperature profile with depth on the right y-axis and water temperatures color coded according to scale in panel c); b) daily precipitation (blue bars) and lake water level (red line; the grey dotted line shows the mean water level); c) differential CO_2 concentration (color code: surface water temperature; color code scale from 4 °C (blue) to 25 °C (yellow)); d) half-hourly CO_2 exchange across the air-water interface with the shaded light blue area marking the period with ice cover.

3.2. Local wind system

Daily average wind speed measured at the east shore ranged from 0.2 to 6 m s^{-1}. At both measurement sites, typical diel variations in wind speed and direction were observed reflecting the thermo-/topographic setting of the lake (Figure 1, Figure 3). During night, westerly and easterly drainage flows converging to the lake were observed at the west and east shore, respectively (Figure 3; dark grey shaded area). After sunrise, a lake breeze (divergence at lake level) developed with onshore flows recorded at both sites (Figure 3; light blue area). On the west shore, the onshore, north-easterly wind persisted between 08:00 and 10:00h local time. Around noon, the up-valley, westerly flow was fully established, replacing the onshore breeze on the west shore and intensifying the westerly wind on the east shore (Figure 3; light grey area). After sunset, the nocturnal drainage flows re-established.

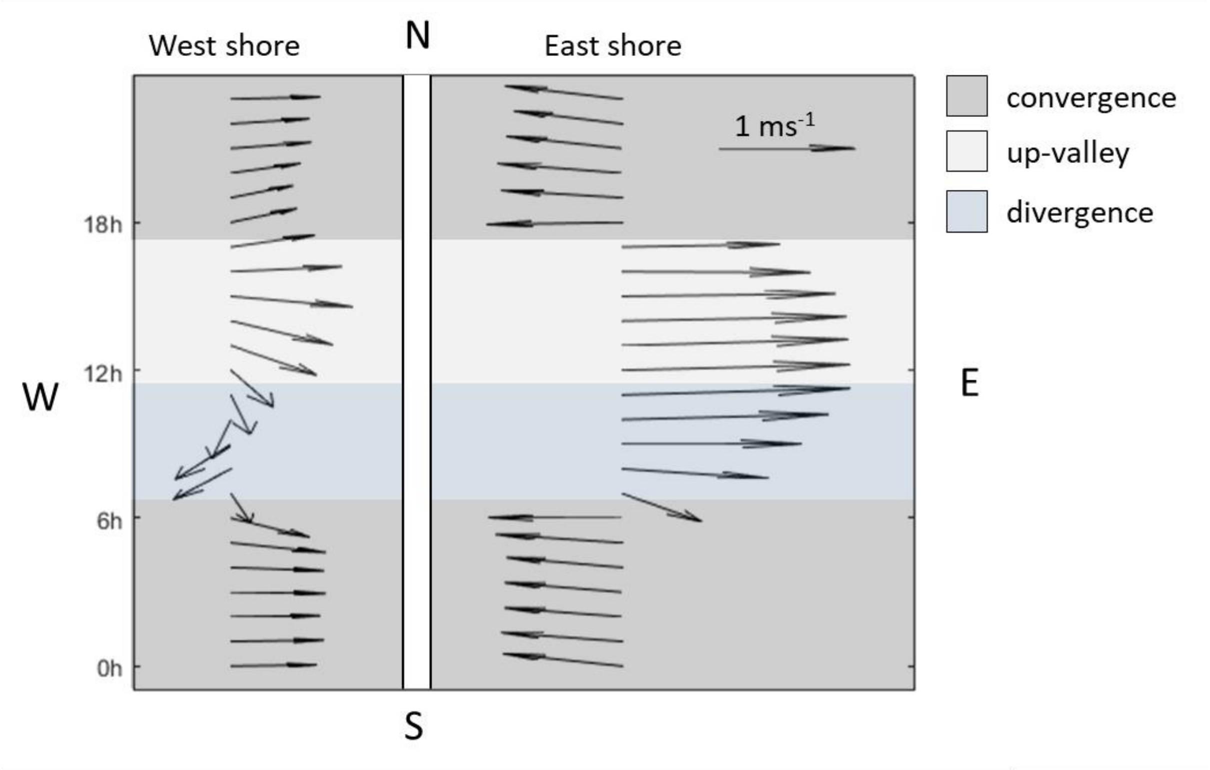

Figure 3 Mean diel variation of wind speed and direction at the opposing shores of the lake. Different shaded areas indicate converging, diverging, and up-valley wind patterns during the respective hours of the day.

We also observed days when the lake breeze persisted throughout the day or when the westerly wind dominated the entire day and in some cases even throughout the night. The former cases were most frequent in August and characterized by very warm temperatures and low wind speeds, while the latter showed generally higher wind speeds than typical days, often during storms with precipitation.

The EC method only measures an upwind signal. Therefore, following our data-analysis, lake fluxes at the east shore were only attributed when the wind was blowing form the west, that is, during times when a lake breeze or up-valley, westerly flows persisted.

3.3. Atmospheric and near-surface water CO_2 concentrations

During the summer months (June-August), the atmospheric CO_2 concentration generally showed a strong diel pattern with high values during the night and lower values during the day. The CO_2 concentrations were highest in the early morning with around 460 ppm on average. After sunrise, the concentration decreased rapidly and stayed around 400 ppm throughout the day. After sunset and as soon as the nocturnal drainage flow established, the CO_2 concentration started to increase again. Interestingly, on days when no nocturnal drainage flow was observed and the westerly wind persisted, the CO_2 concentration stayed low also throughout the night. An example of a typical day (doy 165; diel wind pattern) and a day with persisting westerly winds (doy 168) are depicted in Figure 4.

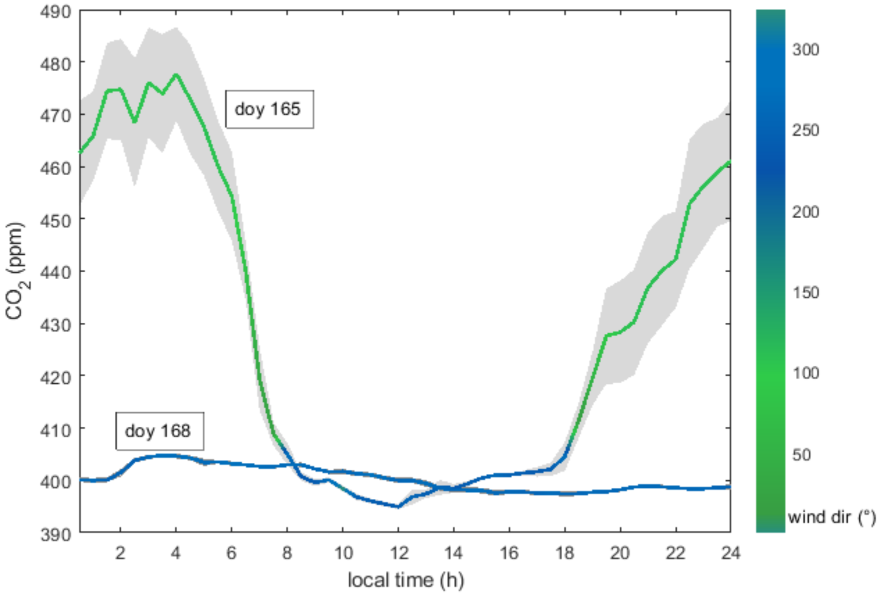

Figure 4 Mean diel variation of atmospheric CO_2 concentration during a typical day (doy 165) and a day when the westerly wind persisted (doy 168). The color indicates the wind direction at the EC station, where green shades represent wind from the land and blue from the lake.

Dissolved CO_2 in the epilimnion also showed a diel pattern, however, with a lower or even reversed amplitude compared to the atmospheric concentration (Figure 5, upper panels). Therefore, the difference in the CO_2 concentration at the air-water interface, ΔCO_2, was low and sometimes negative at night and usually had its maximum around midday (Figure 5, lower panels). However, during times when the wind at the east shore was blowing from the lake (i.e., times when the air-water CO_2 exchange could be measured with the EC set-up), ΔCO_2 showed no or a reverse diel pattern. During those times, the night-time mean ΔCO_2 was mostly higher than the mean ΔCO_2 when data from all wind directions were considered (Figure 5, lower panels).

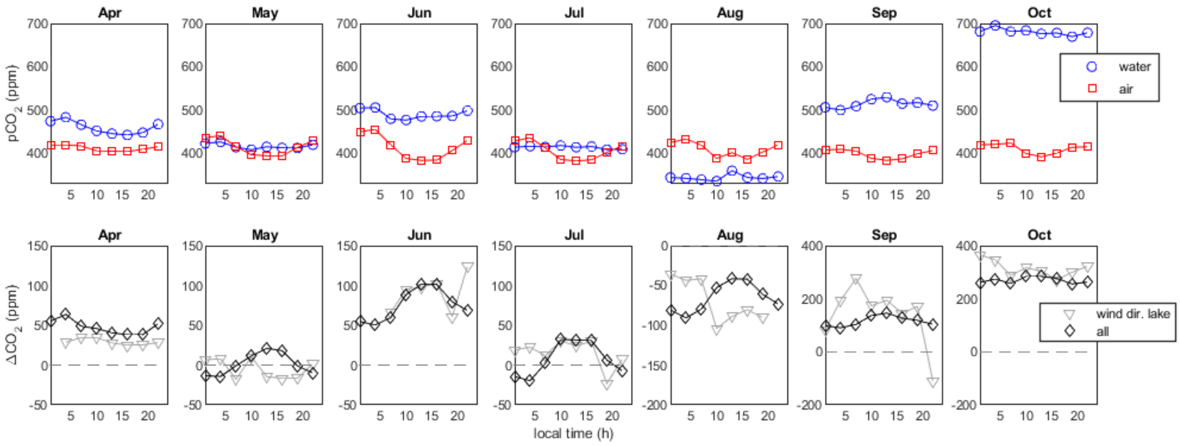

Figure 5 Monthly mean diel variation of CO_2 concentrations of water and air (upper panels) and ΔCO_2 averaged over all times and over times only when the wind was blowing from the lake, respectively (lower panels).

On average, the lake was supersaturated with CO_2 in all months except for August. In May and July, it was very close to equilibrium and several periods of undersaturation were observed (Figure 2c). The rain/cooling events in July generally led to a short-term decrease in surface water CO_2 concentration. In the beginning of August, the CO_2 concentration increased before dropping below atmospheric equilibrium for the rest of the month. The mixing of the water column induced by the heavy rain in the beginning of September eventually led to a strong increase in surface water CO_2 concentration and despite some fluctuations it continuously stayed above atmospheric concentrations afterwards. By the end of the measurements at the end of October, the water concentration exceeded atmospheric concentrations by more than 500 ppm (or 30 µmol L^{-1}) (Figure 2d).

3.4. Directly measured CO_2 fluxes

Estimating CO_2 fluxes by the standard EC method showed generally small fluxes with high short-term temporal variation. Analyzing the respective co-spectra and ogives revealed often large and variable contributions in the low-frequency range. No clear spectral gap could be determined making it difficult to exclude low-frequency contributions based on a fixed averaging time. The application of the OgO method (Text S1; Figure S1) helped to reduce scatter and reveal flux patterns (Figure S2 and S3). Comparing both results (i.e., from the conventional EC and the OgO method) showed that largest discrepancies occurred during lake-breeze and low wind conditions (Figure S4).

In the following, direct flux estimates based on the OgO method are presented. Overall, the lake acted as a net source of CO_2 with an overall mean (± 1 std) emission rate of 0.25 (± 0.36) µmol m^{-2} s^{-1}. For the direct flux measurements, no clear diel variation was observed while fluxes showed seasonal variability with a generally increasing trend towards fall (Figure 6). Highest monthly mean fluxes were observed in October which then decreased slightly towards the end of the year. During the ice free period, April, May, and July showed on average the lowest fluxes. During those months, several periods of C uptake could be observed (Figure 2d), which coincided with cooling of the surface water temperature and rain events on the same or previous days.

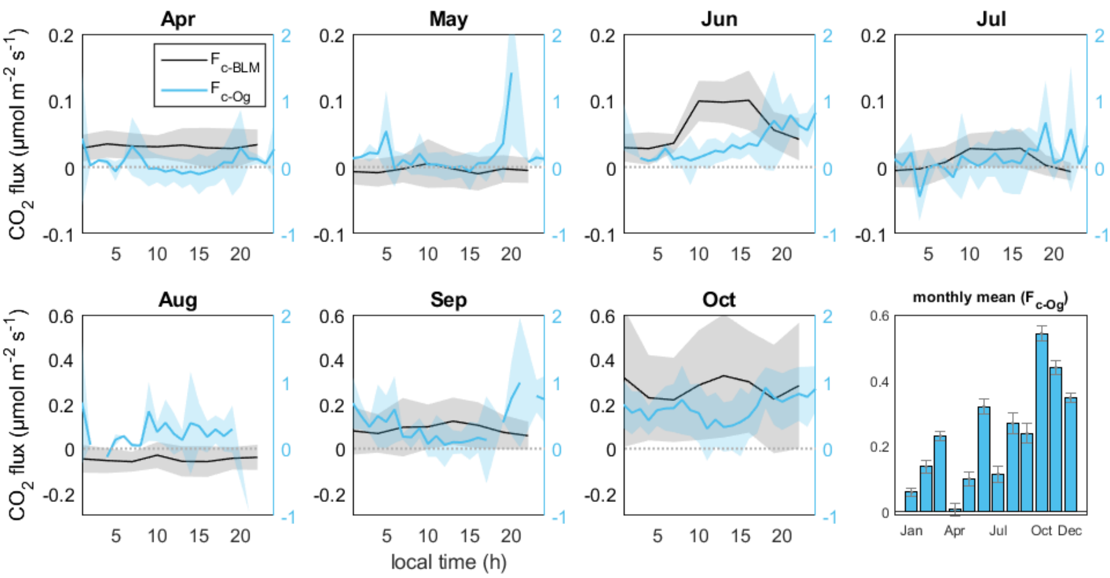

Figure 6 Mean diel variation of $F_{C\text{-}BLM}$ (black lines) and $F_{C\text{-}Og}$ (blue lines) for each month. Shaded areas depict ±1σ. Note the different scales of the y-axes. Monthly mean values (±1 SE) of $F_{C\text{-}Og}$ for the entire year are shown in the lower right panel.

3.5. Gas transfer velocity and BLM CO_2 fluxes

We obtained a linear model for our measured k_{600} values across different wind speeds (U_{10}). The best fit model (±SE) to the data was (equation 8):

$$k_{600}modeled = 2.27(\pm 0.59) * U_{10} + 3.68(\pm 2.97); \quad R^2 = 0.68 \text{ (Figure 7)} \tag{8}$$

We compared our measured k_{600} values and the results of k_{600}modeled with values obtained by three commonly used wind speed based models present in the literature: Cole and Caraco (1998; C&C), Crusius and Wanninkhof (2003; C&W), and Jonsson (2008; J). In the wind range from 0 to ~6 m s^{-1}, we observed an overall underestimation of the model by C&C and C&W, although being within the confidence intervals for very low wind speeds. Despite still being lower than our linear model, the J model was closer and within our confidence intervals. Also, the median binned data confirmed the overall underestimation especially of the C&C model at the given wind speed for this mountain lake system. This detailed comparison is depicted in Figure 7.

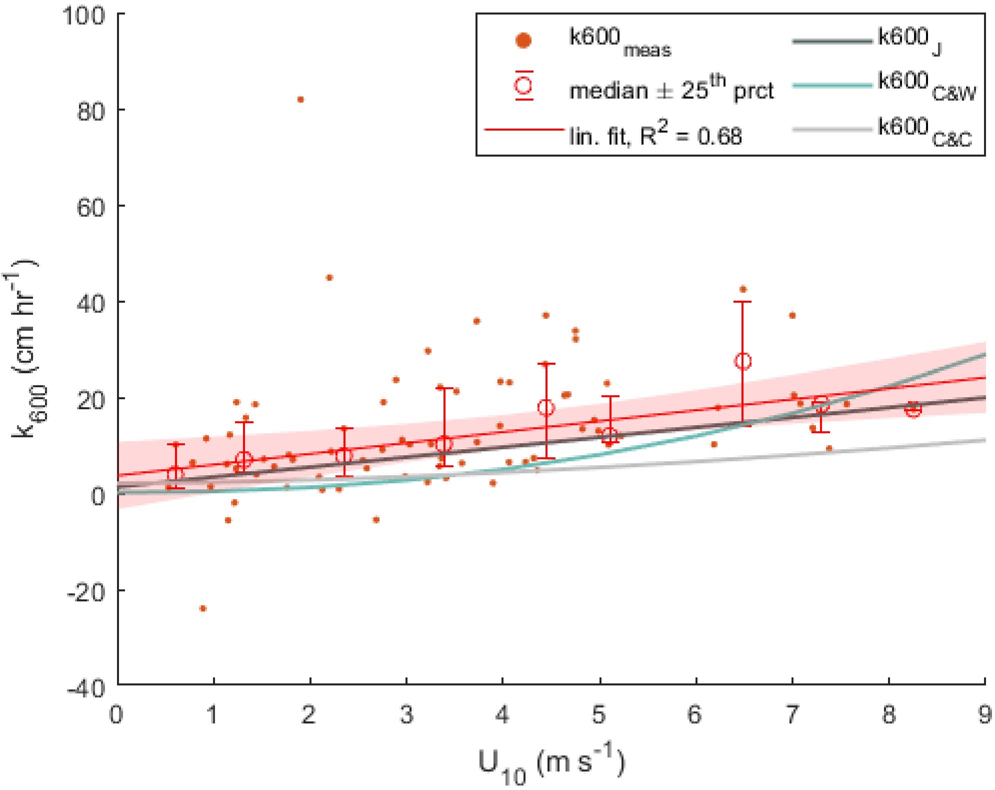

Figure 7 Estimated k600 as a function of U_{10}. Shown are measured k600 values (red dots), median binned data (red circles with the error bars denoting ± 25th percentile), and the best linear fit to the data (red line with confidence intervals denoted by the shaded area). For comparison, previously established k600 models are also shown.

CO_2 fluxes $F_{C\text{-}BLM}$ resulting from the gas transfer model showed a diel trend especially during summer (June, July) and fall (September, October) with higher fluxes during daytime (Figure 6).

Overall, the average (± 1 std) flux from the BLM method was 0.06 (± 0.15) μmol m^{-2} s^{-1}, which is substantially lower than the average directly measured flux $F_{C\text{-}Og}$. It should be noted, however, that the CO_2 flux from the lake can only be measured directly with the EC method when the wind is blowing from the lake. When we averaged only fluxes during times when the wind was blowing from the lake, the value for $F_{C\text{-}BLM}$ increased to 0.13 μmol m^{-2} s^{-1}. Monthly mean fluxes calculated with the

BLM method further showed that the lake acted as a source of atmospheric CO_2 during most months. This monthly CO_2 evasion estimate was always lower than monthly mean $F_{C\text{-}Og}$ and even negative in May and August (Figure 8). Highest fluxes were observed in October independent of the chosen calculation method.

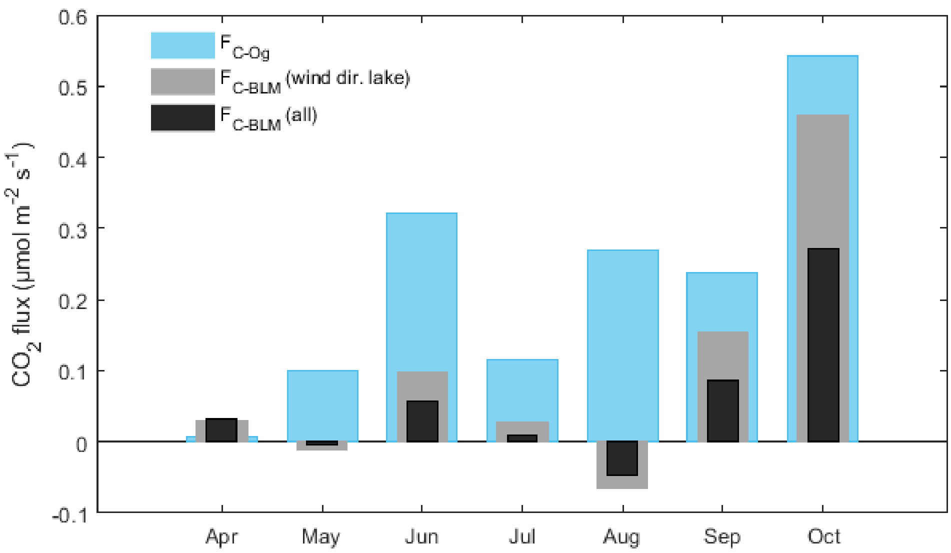

Figure 8 Monthly mean CO_2 fluxes estimated with the EC-OgO method (blue), BLM modeled fluxes for times only when the wind was blowing from the lake (grey), and BLM modeled fluxes for all wind directions (black).

4. Discussion

Wind speed and direction, atmospheric and surface water CO_2 concentrations, and air-water CO_2 exchange were measured at a small mountain lake situated in a narrow, steep valley of the eastern European Alps. Simultaneous wind measurements on opposing shores of the lake revealed the existence of a local wind regime that, together with seasonal variations of CO_2 concentrations in the lake water column, predominantly controlled the variation in lake-atmosphere CO_2 exchange.

We observed a land breeze during night-time and the development of a lake breeze in the morning. During night, lakes often are warmer than the surrounding land promoting the rise of air masses above the lake and drawing in cooler air from the surrounding land. Especially in mountainous regions, lakes – as in our case – are often surrounded by steep hills and therefore represent a relative low point within the area. In sloping terrain, nocturnal down-slope drainage flows are common

(Aubinet et al., 2005; Pypker et al., 2007) which enhance the effect of the land breeze. Drainage of cold air is also associated with drainage of CO_2 from terrestrial ecosystem respiration (Aubinet et al., 2005; Kang et al., 2017). This pattern can also be observed in our dataset, where a significant increase of the atmospheric CO_2 concentration occurred as soon as the wind turned from onshore to offshore. Since the air-water CO_2 exchange is diffusion-driven and dependent on the lake-atmosphere CO_2 concentration difference, a sudden increase of atmospheric CO_2 concentration can transiently suppress CO_2 emissions from the lake, or may even lead to temporary CO_2 uptake. Direct EC measurements of CO_2 fluxes did not reveal a diel pattern of lake-atmosphere CO_2 exchange. Instead, night-time fluxes were the same order of magnitude and occasionally even higher than during daytime and barely showed night-time CO_2 uptake. EC measurements, however, are dependent on wind direction. Since our EC set-up was located on the east shore of the lake, fluxes from the lake could only be measured when westerly winds persisted. Due to the given thermo-topographic conditions this was the case primarily during daytime, although occasionally the wind was blowing from the lake also during night. Nocturnal onshore wind was characterized by comparatively high wind speeds. During those conditions, the nocturnal increase in atmospheric CO_2 concentration and the resulting decrease of ΔCO_2 were not observed, likely due to the absence of drainage flows and better atmospheric mixing during strong westerly winds. Consequently, a decrease in lake-atmosphere CO_2 fluxes is not expected during those nights.

Continuous measurements of CO_2 concentrations in the air and in the surface water allowed calculating the fluxes based on modeled gas transfer velocities. Those results revealed a diel trend of CO_2 exchange with higher fluxes during the day. Moreover, the results demonstrated that direct EC flux measurements, only taken during times when wind conditions allowed the lake to be the source area for the flux, are likely biased by the missing lower fluxes. In our case, direct EC flux measurements resulted in an overestimation of the mean CO_2 efflux form the lake to the atmosphere. This is crucial to consider when measuring lake-atmosphere CO_2 exchange using the EC method in lakes and is especially critical if the measurements are performed from the shore of the lake. Considering flux estimates based on modeled k, our study demonstrates the importance of local atmospheric CO_2 concentration and its temporal variability. In non EC-studies, fluxes are often calculated by assuming a constant average atmospheric pCO_2. However, especially when surface water concentrations are close to equilibrium, small temporal and local differences in atmospheric CO_2 can determine the lake being a source or sink for CO_2.

Although both $F_{C\text{-}Og}$ and $F_{C\text{-}BLM}$ indicated that the lake on average was a small source of CO_2 discrepancies between the two methods remained. $F_{C\text{-}BLM}$ was consistently lower than $F_{C\text{-}Og}$, which previously was observed in other studies (Erkkilä et al., 2018; Huotari et al., 2011; Mammarella et al., 2015) and primarily attributed to uncertainties in the estimation of k. In our case, part of the discrepancies was probably caused by a diel bias in EC measurements. However, differences remained even after accounting for this bias and were most pronounced in August when a negative ΔCO_2 implied CO_2 uptake, while $F_{C\text{-}Og}$ suggested a CO_2 release. This discrepancy could be caused by spatial variability of CO_2 fluxes because the two methods generally differ in spatial resolution and in our case also covered different parts of the lake. The EC set-up was on the shore, therefore $F_{C\text{-}Og}$ represents fluxes from shallow waters. On the other hand, C_w, which was used to calculate $F_{C\text{-}BLM}$, was measured near the center, at the deepest point of the lake. Other studies have also observed within lake spatial variability of F_c and C_w (Kelly et al., 2001; Loken et al., 2019) and often reported higher values for shallow water. For example, EC measurements at a Finish lake showed higher fluxes when the footprint was above shallower water (Erkkilä et al., 2018). Spafford and Risk (2018) used floating chambers to measure F_c along a transect in the littoral zone and found higher and more variable fluxes closest to the shore. Shallow water might be warmer and therefore increase microbial respiration and the resulting emission of CO_2. Moreover, sediments are closer to the water surface and the mixing layer can extend all the way to the lake bed more easily. Close to the shore, organic material from the surrounding land can enter the water and directly provide decomposable substrate for microbial respiration. In addition, surface water and hyporheic CO_2 inflows (Peter et al., 2014) will also have a higher effect on lake water CO_2 closer to the shore.

Although the applied OgO method provides a tool to reduce low-frequency impact on direct flux measurements, non-turbulent contributions to the estimated fluxes cannot be completely precluded. This, as well as uncertainty in the estimation of k, can be an additional cause for the observed discrepancies between the methods.

Nevertheless, results from both methods showed in general a similar seasonal pattern. Fluxes were low in spring and in contrast to other studies no bursts of CO_2 were observed during ice out (Ducharme-Riel et al., 2015; Huotari et al., 2011; Karlsson et al., 2013), although, on average, fluxes were higher in March than in January and February. On average, the lake acted as a net source of CO_2 also during the summer month. Nevertheless, several periods of CO_2 uptake were observed especially in July and overall the variability of CO_2 fluxes was high. Frequent undersaturation and CO_2 uptake has been observed in other studies as well, especially for eutrophic lakes (Balmer and Downing, 2011). In our study, however, this could not be explained unequivocally by biological activity of primary producers. Instead, periods of CO_2 uptake were rather associated with temporal cooling of air and consequently surface water temperature and, most of the time, light rainfall. Nevertheless, given that primary production in lakes often is determined by limiting nutrients (Prairie and Cole, 2009), we hypothesize that the light rainfall may also have enhanced productivity by increasing nutrient availability through enhanced fluvial inflow or partial mixing of the lake water column, while the colder temperatures temporary decreased respiration. Previously, cooling of lake surface temperature was observed to increase lake-atmosphere C fluxes by enhancing convective mixing (Eugster et al., 2003). However, in our case, C_w was rather low and the cooling of the water may have led to a significant increase in CO_2 solubility. In addition, direct input of rainwater could have caused an additional dilution effect at the surface. In contrast, heavy rain events, as indicated by a marked increase of lake water level, were generally followed by an increase in C_w and also F_c – most pronounced at the beginning of August and at the beginning of September. In those cases, runoff from the catchment probably led to an increased organic and inorganic C load (Ejarque et al., 2021). In the beginning of September, the heavy precipitation event likely also caused upwelling of

CO_2 rich water. Afterwards, C_w stayed high and highest fluxes were eventually observed in October due to several storm events with very high wind speeds. This implies that physical, rather than biological, factors drive CO_2 emissions at this small mountain lake.

Direct EC CO_2 flux measurements indicated that Lake Lunz, on average, emitted 0.25 µmol m^{-2} s^{-1} equivalent to 259 mg C m^{-2} d^{-1}. This is likely an overestimation, as an average flux of 0.06 µmol m^{-2} s^{-1} or 62 mg C m^{-2} d^{-1} was estimated using the BLM method.

Our results are within the range of reported results from EC measurements at lakes in different regions (Table 1). It should be noted, however, that to the authors' knowledge no comparable long-term direct measurements from Alpine lakes exist. Also, direct comparison of the measured fluxes to other lakes is difficult due to different time frames, instrumentation, and flux processing (detailed information on instrumentation and data processing as reported in the respective papers is given in Table S1 in the supporting information). Most of the conducted studies were short-term measurements focusing on spring or fall turnover. Multi-year investigations are predominantly from northern boreal regions and usually include only the ice-free periods. Overall, this demonstrates that continuous, long-term, direct flux measurements at lake ecosystems and a coherent flux processing strategy for those systems are still lacking.

EC measurements at lakes pose several challenges. First, the choice for the site of instrument set-up is crucial. Several studies were conducted from floating platforms being advantageous in terms of land influence and acceptable wind directions. However, the movement of the platform might influence not only the wind measurements (Eugster et al., 2003) but also gas analyzers (Eugster et al., 2020) and other instruments might be sensitive to motion and this has to be considered in data processing. Set up on shore provides easier handling and maintenance but, as shown in our case, might be prone to biased data collection because only certain wind directions can be accepted. By choosing a site, also downwind conditions have to be considered as sharp surface transitions (e.g., lake to forest) can influence the wind field (Kenny et al., 2017). High scatter and unrealistic flux values are commonly observed in aquatic EC flux measurements independent of the chosen instruments or measurement location (e.g. Czikowsky et al., 2018; Eugster et al., 2003; Liu et al., 2016). Causes for those observations can be advection, influence from the surrounding land or, more generally, low-frequency contributions. For terrestrial ecosystems, stable, low wind conditions are known to be challenging, concerning especially night-time flux quantification (Aubinet, 2008). For lakes, large influence from non-local processes has also been observed for high wind speeds (Esters et al., 2020). Yet overall, we could not determine any generalized condition, under which the unrealistic flux values occurred.

In the past, this issue has been addressed with different solutions, for example by shorter averaging times (Eugster et al., 2003; Vesala et al., 2006), more stringent thresholds for quality criteria (Czikowsky et al., 2018; Huotari et al., 2011), or rigorous outlier removal (Franz et al., 2016). Our data also showed unrealistic large fluxes and variability. Although an extensive (raw) data analysis naturally showed that low wind and low flux conditions are critical, unrealistic flux values were also observed with shorter averaging intervals and under preferable wind conditions and with the footprint entirely above the lake surface. An ogive analysis revealed considerable low-frequency contribution to the measured CO_2 flux in many cases and an estimation of the flux using the recently developed OgO method, therefore, appeared most robust.

Table 1: Overview of EC CO_2 flux measurements at lakes

Reference	Lake/Location	Time frame	Flux (mg C m^{-2} d^{-1})
our study	Lake Lunz, Austria	1 year (2017)	259
(Anderson et al., 1999)	Williams Lake, MN, USA	5x1 week (spring/summer/fall)	-186 to 2800
(Armani et al., 2020)	Itaipu Lake, Brazil	Jan - Nov 2013 (non-continuous)	301
(Czikowsky et al., 2018)	Lake Pleasant, NY, USA	16. Sept - 11. Oct 2010	348
(Du et al., 2018)	Erhai Lake, China	2012 - 2015	322 to 443
(Erkkilä et al., 2018)	Lake Kuivajärvi, Finnland	fall 2014 (16 days)	363 to 1130
(Eugster et al., 2003)	Toolik Lake, AK, USA	short term (2-4 days in July)	114
(Eugster et al., 2003)	Soppensee, Switzerland	short term (3 days in September)	289
(Eugster et al., 2020)	Toolik Lake, AK, USA	ice free periods 2010-2015	200
(Franz et al., 2016)	Polder Zarnekow, Germany	May 2013 - May 2014	118
(Han et al., 2020)	Ngoring Lake, Tibet	ice free periods 2011-2013	-830 to 130
(Huotari et al., 2011), see also (Vesala et al., 2006)	Lake Valkea-Kotinen, Finland	ice free periods 2003-2007	210 (186 to 266)
(Jammet et al., 2017)	Villasjön, Sweden	Jun 2012 - Dec 2014	228
(Jonsson et al., 2008)	Lake Merasjärvi, Sweden	Jun - Okt 2005	221
(Kim et al., 2016)	Eastmain-1 reservoir, Canada	ice free periods 2006-2009	1140
(Liu et al., 2015)	Erhai Lake, China	1 year (2012)	466 to 1284
(Liu et al., 2016)	Ross Barnett Reservoir, MS, USA	1 year (2008)	321
(Lohila et al., 2015)	Pallasjärv, Finland	Jul-Oct 2013	210
(Mammarella et al., 2015); see also (Heiskanen et al., 2014)	Lake Kuivajärvi, Finland	Jun - Oct 2010 & 2011	726
(Morin et al., 2017)	Douglas Lake, MI, USA	Jun - Sept/Oct 2013 & 2014	726
(Podgrajsek et al., 2015)	Lake Tämnaren, Sweden	Sept 2010 - Sept 2012	187
(Polsenaere et al., 2013)	Floodplain lake, Barzil	19.-22.Nov 2011	612
(Potes et al., 2017)	Alqueva reservoir, Portugal	2. Jun-2. Oct 2014	-38
(Reed et al., 2018)	Lake Mendota, WI, USA	2012-2017	-151 to -636
(Shao et al., 2015) see also (Ouyang et al., 2017)	Lake Erie, USA	Oct 2011 - Sept 2013	173
(Sollberger et al., 2017)	Lake Klöntal, Switzerland	Mar - Jun 2012	15.5

5. Conclusion

Direct measurements of CO_2 exchange between a small lake and the atmosphere were conducted and related to the temporal variability of atmospheric and surface water CO_2 concentrations and meteorological conditions. The lake acted as a small source of CO_2, showing distinct seasonal and diel patterns of CO_2 fluxes. Spring and summer fluxes were low and highest fluxes were observed in October after partial lake mixing. Several CO_2 uptake periods were observed, usually during cold and rainy weather and likely driven by physical rather than biological factors. Fluxes calculated using the BLM method showed a diel pattern with lower fluxes during the night. Drainage flows from the surrounding land and low wind speeds during night led to increased atmospheric CO_2 and in consequence decreased ΔCO_2 resulting in reduced CO_2 emissions or even CO_2 uptake by the lake. This pattern was lacking in the results of the EC flux measurements due to the instrument deployment on the shore of the lake and the local wind system. In general, we propose that the influence of the surrounding landscape needs to be addressed when measuring lake-atmosphere fluxes, especially when fluxes are small and when dealing with lakes situated in complex topography.

Acknowledgements

This study was supported by the Austrian Academy of Sciences (ÖAW) as part of the project ‘Influence of climate extremes on C cycling dynamics across the boundaries of aquatic ecosystems (EXCARB)’ and by the Autonome Provinz Bozen-Südtirol (ALCH4 Project). We would like to thank Michael Mayr, Christian Preiler, and other people at the Wasser Cluster Lunz for help on data acquisition, instrument maintenance, and logistical support. We would like to thank the Austrian Central Institution for Meteorology and Geodynamics (ZAMG) and the Hydrographic Service of Lower Austria for data provision. Thanks to J. Sievers for developing and providing the Ogive Optimization Toolbox. The authors declare that they have no conflict of interest. Data presented and analyzed in this work is available online at https://doi.org/10.5281/zenodo.4519167.

References

Anderson, D.E., Striegl, R.G., Stannard, D.I., Michmerhuizen, C.M., McConnaughey, T.A., LaBaugh, J.W., 1999. Estimating lake-atmosphere CO_2 exchange. Limnol. Oceanogr. 44, 988–1001. https://doi.org/10.4319/lo.1999.44.4.0988

Armani, F.A.S., Dias, N.L., Damázio, J.M., Armani, F.A.S., Dias, N.L., Damázio, J.M., 2020. Eddy-covariance CO_2 fluxes over Itaipu lake, southern Brazil. RBRH 25. https://doi.org/10.1590/2318-0331.252020200060

Aubinet, M., 2008. Eddy Covariance CO_2 Flux Measurements in Nocturnal Conditions: An Analysis of the Problem. Ecological Applications 18, 1368–1378. https://doi.org/10.1890/06-1336.1

Aubinet, M., Berbigier, P., Bernhofer, Ch., Cescatti, A., Feigenwinter, C., Granier, A., Grünwald, Th., Havrankova, K., Heinesch, B., Longdoz, B., Marcolla, B., Montagnani, L., Sedlak, P., 2005. Comparing CO_2 Storage and Advection Conditions at Night at Different Carboeuroflux Sites. Boundary-Layer Meteorology 116, 63–93. https://doi.org/10.1007/s10546-004-7091-8

Aubinet, M., Vesala, T., Papale, D., 2012. Eddy Covariance. Springer Netherlands, Dordrecht.

Aufdenkampe, A.K., Mayorga, E., Raymond, P.A., Melack, J.M., Doney, S.C., Alin, S.R., Aalto, R.E., Yoo, K., 2011. Riverine coupling of biogeochemical cycles between land, oceans, and atmosphere. Frontiers in Ecology and the Environment 9, 53–60. https://doi.org/10.1890/100014

Baldocchi, D., 2014. Measuring fluxes of trace gases and energy between ecosystems and the atmosphere – the state and future of the eddy covariance method. Glob Change Biol 20, 3600–3609. https://doi.org/10.1111/gcb.12649

Baldocchi, D.D., Hincks, B.B., Meyers, T.P., 1988. Measuring Biosphere-Atmosphere Exchanges of Biologically Related Gases with Micrometeorological Methods. Ecology 69, 1331–1340. https://doi.org/10.2307/1941631

Balmer, M.B., Downing, J.A., 2011. Carbon dioxide concentrations in eutrophic lakes: undersaturation implies atmospheric uptake. Inland Waters 1, 125–132. https://doi.org/10.5268/IW-1.2.366

Bastviken, D., Cole, J., Pace, M., Tranvik, L., 2004. Methane emissions from lakes: Dependence of lake characteristics, two regional assessments, and a global estimate. Global Biogeochemical Cycles 18. https://doi.org/10.1029/2004GB002238

Bastviken, D., Sundgren, I., Natchimuthu, S., Reyier, H., Gålfalk, M., 2015. Technical Note: Cost-efficient approaches to measure carbon dioxide (CO_2) fluxes and concentrations in terrestrial and aquatic environments using mini loggers. Biogeosciences 12, 3849–3859. https://doi.org/10.5194/bg-12-3849-2015

Battin, T.J., Luyssaert, S., Kaplan, L.A., Aufdenkampe, A.K., Richter, A., Tranvik, L.J., 2009. The boundless carbon cycle. Nature Geosci 2, 598–600. https://doi.org/10.1038/ngeo618

Bischoff-Gauß, I., Kalthoff, N., Fiebig-Wittmaack, M., 2006. The influence of a storage lake in the Arid Elqui Valley in Chile on local climate. Theor. Appl. Climatol. 85, 227–241. https://doi.org/10.1007/s00704-005-0190-8

Blöschl, G., Hall, J., Viglione, A., Perdigão, R.A.P., Parajka, J., Merz, B., Lun, D., Arheimer, B., Aronica, G.T., Bilibashi, A., Boháč, M., Bonacci, O., Borga, M., Čanjevac, I., Castellarin, A., Chirico, G.B., Claps, P., Frolova, N., Ganora, D., Gorbachova, L., Gül, A., Hannaford, J., Harrigan, S., Kireeva, M., Kiss, A., Kjeldsen, T.R., Kohnová, S., Koskela, J.J., Ledvinka, O., Macdonald, N., Mavrova-Guirguinova, M., Mediero, L., Merz, R., Molnar, P., Montanari, A., Murphy, C., Osuch, M., Ovcharuk, V., Radevski, I., Salinas, J.L., Sauquet, E., Šraj, M., Szolgay, J., Volpi, E., Wilson, D., Zaimi, K., Živković, N., 2019. Changing climate both increases and decreases European river floods. Nature 573, 108–111. https://doi.org/10.1038/s41586-019-1495-6

Ciais, P., Sabine, C., Bala, G., Bopp, L., Brovkin, V., Canadell, J., Chhabra, A., DeFries, R., Galloway, J., Heimann, M., Jones, C., Le Quéré, C., Myneni, R.B., Piao, S., Thornton, P., 2013. Carbon and Other Biogeochemical Cycles., in: Climate Change 2013: The Physical Science Basis. Contribution of Working Group I to the Fifth Assessment Report of the Intergovernmental Panel on Climate Change. Cambridge University Press, Cambridge, United Kingdom and New York, NY, USA.

Cole, J.J., Caraco, N.F., 1998. Atmospheric exchange of carbon dioxide in a low-wind oligotrophic lake measured by the addition of SF6. Limnol. Oceanogr. 43, 647–656.
Cole, J.J., Caraco, N.F., Kling, G.W., Kratz, T.K., 1994. Carbon Dioxide Supersaturation in the Surface Waters of Lakes. Science 265, 1568–1570.
Cole, J.J., Prairie, Y.T., Caraco, N.F., McDowell, W.H., Tranvik, L.J., Striegl, R.G., Duarte, C.M., Kortelainen, P., Downing, J.A., Middelburg, J.J., Melack, J., 2007. Plumbing the Global Carbon Cycle: Integrating Inland Waters into the Terrestrial Carbon Budget. Ecosystems 10, 172–185. https://doi.org/10.1007/s10021-006-9013-8
Crawford, J.T., Loken, L.C., Casson, N.J., Smith, C., Stone, A.G., Winslow, L.A., 2015. High-Speed Limnology: Using Advanced Sensors to Investigate Spatial Variability in Biogeochemistry and Hydrology. Environ. Sci. Technol. 49, 442–450. https://doi.org/10.1021/es504773x
Crusius, J., Wanninkhof, R., 2003. Gas transfer velocities measured at low wind speed over a lake. Limnology and Oceanography 48, 1010–1017. https://doi.org/10.4319/lo.2003.48.3.1010
Czikowsky, M.J., MacIntyre, S., Tedford, E.W., Vidal, J., Miller, S.D., 2018. Effects of Wind and Buoyancy on Carbon Dioxide Distribution and Air-Water Flux of a Stratified Temperate Lake. Journal of Geophysical Research: Biogeosciences 123, 2305–2322. https://doi.org/10.1029/2017JG004209
Drake, T.W., Raymond, P.A., Spencer, R.G.M., 2018. Terrestrial carbon inputs to inland waters: A current synthesis of estimates and uncertainty. Limnology and Oceanography Letters 3, 132–142. https://doi.org/10.1002/lol2.10055
Du, Q., Liu, H.Z., Liu, Y., Wang, L., Xu, L.J., Sun, J.H., Xu, A.L., 2018. Factors controlling evaporation and the CO_2 flux over an open water lake in southwest of China on multiple temporal scales. International Journal of Climatology 38, 4723–4739. https://doi.org/10.1002/joc.5692
Ducharme-Riel, V., Vachon, D., del Giorgio, P.A., Prairie, Y.T., 2015. The Relative Contribution of Winter Under-Ice and Summer Hypolimnetic CO_2 Accumulation to the Annual CO_2 Emissions from Northern Lakes. Ecosystems 18, 547–559. https://doi.org/10.1007/s10021-015-9846-0
Ejarque, E., Scholz, K., Wohlfahrt, G., Battin, T.J., Kainz, M.J., Schelker, J., 2021. Hydrology controls the carbon mass balance of a mountain lake in the eastern European Alps. Limnology and Oceanography. https://doi.org/10.1002/lno.11712
Erkkilä, K.-M., Ojala, A., Bastviken, D., Biermann, T., Heiskanen, J.J., Lindroth, A., Peltola, O., Rantakari, M., Vesala, T., Mammarella, I., 2018. Methane and carbon dioxide fluxes over a lake: comparison between eddy covariance, floating chambers and boundary layer method. Biogeosciences 15, 429–445. https://doi.org/10.5194/bg-15-429-2018
Esters, L., Rutgersson, A., Nilsson, E., Sahlée, E., 2020. Non-local Impacts on Eddy-Covariance Air–Lake CO_2 Fluxes. Boundary-Layer Meteorol. https://doi.org/10.1007/s10546-020-00565-2
Eugster, W., DelSontro, T., Shaver, G.R., Kling, G.W., 2020. Interannual, summer, and diel variability of CH_4 and CO_2 effluxes from Toolik Lake, Alaska, during the ice-free periods 2010–2015. Environ. Sci.: Processes Impacts 22, 2181–2198. https://doi.org/10.1039/D0EM00125B
Eugster, W., Kling, G., Jonas, T., McFadden, J.P., Wüest, A., MacIntyre, S., Chapin, F.S., 2003. CO_2 exchange between air and water in an Arctic Alaskan and midlatitude Swiss lake: Importance of convective mixing. J. Geophys. Res. 108, 4362. https://doi.org/10.1029/2002JD002653
Foken, Th., Wichura, B., 1996. Tools for quality assessment of surface-based flux measurements. Agricultural and Forest Meteorology 78, 83–105. https://doi.org/10.1016/0168-1923(95)02248-1
Franz, D., Koebsch, F., Larmanou, E., Augustin, J., Sachs, T., 2016. High net CO_2 and CH_4 release at a eutrophic shallow lake on a formerly drained fen. Biogeosciences 13, 3051–3070. https://doi.org/10.5194/bg-13-3051-2016
Gobiet, A., Kotlarski, S., Beniston, M., Heinrich, G., Rajczak, J., Stoffel, M., 2014. 21st century climate change in the European Alps—A review. Science of The Total Environment 493, 1138–1151. https://doi.org/10.1016/j.scitotenv.2013.07.050
Han, B., Meng, X., Yang, Q., Wu, R., Lv, S., Li, Z., Wang, X., Li, Y., Yu, L., 2020. Connections Between Daily Surface Temperature Contrast and CO_2 Flux Over a Tibetan Lake: A Case Study of

Ngoring Lake. Journal of Geophysical Research: Atmospheres 125, e2019JD032277. https://doi.org/10.1029/2019JD032277

Hartmann, J., Lauerwald, R., Moosdorf, N., 2014. A Brief Overview of the GLObal RIver Chemistry Database, GLORICH. Procedia Earth and Planetary Science, Geochemistry of the Earth's surface GES-10 Paris France, 18-23 August, 2014. 10, 23–27. https://doi.org/10.1016/j.proeps.2014.08.005

Heiskanen, J.J., Mammarella, I., Haapanala, S., Pumpanen, J., Vesala, T., MacIntyre, S., Ojala, A., 2014. Effects of cooling and internal wave motions on gas transfer coefficients in a boreal lake. Tellus B: Chemical and Physical Meteorology 66, 22827. https://doi.org/10.3402/tellusb.v66.22827

Holgerson, M.A., Raymond, P.A., 2016. Large contribution to inland water CO_2 and CH_4 emissions from very small ponds. Nature Geosci 9, 222–226. https://doi.org/10.1038/ngeo2654

Huotari, J., Ojala, A., Peltomaa, E., Nordbo, A., Launiainen, S., Pumpanen, J., Rasilo, T., Hari, P., Vesala, T., 2011. Long-term direct CO_2 flux measurements over a boreal lake: Five years of eddy covariance data. Geophys. Res. Lett. 38, L18401. https://doi.org/10.1029/2011GL048753

Jähne, B., Münnich, K.O., Bösinger, R., Dutzi, A., Huber, W., Libner, P., 1987. On the parameters influencing air-water gas exchange. Journal of Geophysical Research: Oceans 92, 1937–1949. https://doi.org/10.1029/JC092iC02p01937

Jammet, M., Dengel, S., Kettner, E., Parmentier, F.-J.W., Wik, M., Crill, P., Friborg, T., 2017. Year-round CH_4 and CO_2 flux dynamics in two contrasting freshwater ecosystems of the subarctic. Biogeosciences 14, 5189–5216. https://doi.org/10.5194/bg-14-5189-2017

Jonsson, A., Åberg, J., Lindroth, A., Jansson, M., 2008. Gas transfer rate and CO_2 flux between an unproductive lake and the atmosphere in northern Sweden. J. Geophys. Res. 113, G04006. https://doi.org/10.1029/2008JG000688

Kang, M., Ruddell, B.L., Cho, C., Chun, J., Kim, J., 2017. Identifying CO_2 advection on a hill slope using information flow. Agricultural and Forest Meteorology 232, 265–278. https://doi.org/10.1016/j.agrformet.2016.08.003

Karlsson, J., Giesler, R., Persson, J., Lundin, E., 2013. High emission of carbon dioxide and methane during ice thaw in high latitude lakes. Geophysical Research Letters 40, 1123–1127. https://doi.org/10.1002/grl.50152

Kelly, C.A., Fee, E., Ramlal, P.S., Rudd, J.W.M., Hesslein, R.H., Anema, C., Schindler, E.U., 2001. Natural variability of carbon dioxide and net epilimnetic production in the surface waters of boreal lakes of different sizes. Limnology and Oceanography 46, 1054–1064. https://doi.org/10.4319/lo.2001.46.5.1054

Kenny, W.T., Bohrer, G., Morin, T.H., Vogel, C.S., Matheny, A.M., Desai, A.R., 2017. A Numerical Case Study of the Implications of Secondary Circulations to the Interpretation of Eddy-Covariance Measurements Over Small Lakes. Boundary-Layer Meteorol 165, 311–332. https://doi.org/10.1007/s10546-017-0268-8

Kim, Y., Roulet, N.T., Li, C., Frolking, S., Strachan, I.B., Peng, C., Teodoru, C.R., Prairie, Y.T., Tremblay, A., 2016. Simulating carbon dioxide exchange in boreal ecosystems flooded by reservoirs. Ecological Modelling 327, 1–17. https://doi.org/10.1016/j.ecolmodel.2016.01.006

Klaus, M., Vachon, D., 2020. Challenges of predicting gas transfer velocity from wind measurements over global lakes. Aquat Sci 82, 53. https://doi.org/10.1007/s00027-020-00729-9

Libes, S., 2009. Introduction to Marine Biogeochemistry, 2nd ed. Academic Press.

Liss, P.S., Slater, P.G., 1974. Flux of Gases across the Air-Sea Interface. Nature 247, 181–184. https://doi.org/10.1038/247181a0

Liu, H., Feng, J., Sun, J., Wang, L., Xu, A., 2015. Eddy covariance measurements of water vapor and CO_2 fluxes above the Erhai Lake. Sci. China-Earth Sci. 58, 317–328. https://doi.org/10.1007/s11430-014-4828-1

Liu, H., Zhang, Q., Katul, G.G., Cole, J.J., Chapin, F.S., MacIntyre, S., 2016. Large CO_2 effluxes at night and during synoptic weather events significantly contribute to CO_2 emissions from a reservoir. Environ. Res. Lett. 11, 064001. https://doi.org/10.1088/1748-9326/11/6/064001

Lohila, A., Tuovinen, J.-P., Hatakka, J., Aurela, M., Vuorenmaa, J., Haakana, M., Laurila, T., 2015. Carbon dioxide and energy fluxes over a northern boreal lake. Boreal Environment Research 20, 474–488.

Loken, L.C., Crawford, J.T., Schramm, P.J., Stadler, P., Desai, A.R., Stanley, E.H., 2019. Large Spatial and Temporal Variability of Carbon Dioxide and Methane in a Eutrophic Lake. Journal of Geophysical Research: Biogeosciences 124, 2248–2266. https://doi.org/10.1029/2019JG005186

Lorke, A., Bodmer, P., Noss, C., Alshboul, Z., Koschorreck, M., Somlai-Haase, C., Bastviken, D., Flury, S., McGinnis, D.F., Maeck, A., Müller, D., Premke, K., 2015. Technical note: drifting versus anchored flux chambers for measuring greenhouse gas emissions from running waters. Biogeosciences 12, 7013–7024. https://doi.org/10.5194/bg-12-7013-2015

MacIntyre, S., Jonsson, A., Jansson, M., Aberg, J., Turney, D.E., Miller, S.D., 2010. Buoyancy flux, turbulence, and the gas transfer coefficient in a stratified lake. Geophysical Research Letters 37. https://doi.org/10.1029/2010GL044164

Mammarella, I., Nordbo, A., Rannik, Ü., Haapanala, S., Levula, J., Laakso, H., Ojala, A., Peltola, O., Heiskanen, J., Pumpanen, J., Vesala, T., 2015. Carbon dioxide and energy fluxes over a small boreal lake in Southern Finland. J. Geophys. Res. Biogeosci. 2014JG002873. https://doi.org/10.1002/2014JG002873

Matthews, C.J.D., St.Louis, V.L., Hesslein, R.H., 2003. Comparison of Three Techniques Used To Measure Diffusive Gas Exchange from Sheltered Aquatic Surfaces. Environ. Sci. Technol. 37, 772–780. https://doi.org/10.1021/es0205838

Mendonça, R., Müller, R.A., Clow, D., Verpoorter, C., Raymond, P., Tranvik, L.J., Sobek, S., 2017. Organic carbon burial in global lakes and reservoirs. Nature Communications 8, 1694. https://doi.org/10.1038/s41467-017-01789-6

Morin, T.H., Rey-Sánchez, A.C., Vogel, C.S., Matheny, A.M., Kenny, W.T., Bohrer, G., 2017. Carbon dioxide emissions from an oligotrophic temperate lake: An eddy covariance approach. Ecological Engineering. https://doi.org/10.1016/j.ecoleng.2017.05.005

Ouyang, Z., Shao, C., Chu, H., Becker, R., Bridgeman, T., Stepien, C.A., John, R., Chen, J., 2017. The Effect of Algal Blooms on Carbon Emissions in Western Lake Erie: An Integration of Remote Sensing and Eddy Covariance Measurements. Remote Sensing 9, 44. https://doi.org/10.3390/rs9010044

Pastorello, G., Trotta, C., Canfora, E., Chu, H., Christianson, D., Cheah, Y.-W., Poindexter, C., Chen, J., Elbashandy, A., Humphrey, M., Isaac, P., Polidori, D., Ribeca, A., van Ingen, C., Zhang, L., Amiro, B., Ammann, C., Arain, M.A., Ardö, J., Arkebauer, T., Arndt, S.K., Arriga, N., Aubinet, M., Aurela, M., Baldocchi, D., Barr, A., Beamesderfer, E., Marchesini, L.B., Bergeron, O., Beringer, J., Bernhofer, C., Berveiller, D., Billesbach, D., Black, T.A., Blanken, P.D., Bohrer, G., Boike, J., Bolstad, P.V., Bonal, D., Bonnefond, J.-M., Bowling, D.R., Bracho, R., Brodeur, J., Brümmer, C., Buchmann, N., Burban, B., Burns, S.P., Buysse, P., Cale, P., Cavagna, M., Cellier, P., Chen, S., Chini, I., Christensen, T.R., Cleverly, J., Collalti, A., Consalvo, C., Cook, B.D., Cook, D., Coursolle, C., Cremonese, E., Curtis, P.S., D'Andrea, E., da Rocha, H., Dai, X., Davis, K.J., De Cinti, B., de Grandcourt, A., De Ligne, A., De Oliveira, R.C., Delpierre, N., Desai, A.R., Di Bella, C.M., di Tommasi, P., Dolman, H., Domingo, F., Dong, G., Dore, S., Duce, P., Dufrêne, E., Dunn, A., Dušek, J., Eamus, D., Eichelmann, U., ElKhidir, H.A.M., Eugster, W., Ewenz, C.M., Ewers, B., Famulari, D., Fares, S., Feigenwinter, I., Feitz, A., Fensholt, R., Filippa, G., Fischer, M., Frank, J., Galvagno, M., Gharun, M., Gianelle, D., Gielen, B., Gioli, B., Gitelson, A., Goded, I., Goeckede, M., Goldstein, A.H., Gough, C.M., Goulden, M.L., Graf, A., Griebel, A., Gruening, C., Grünwald, T., Hammerle, A., Han, S., Han, X., Hansen, B.U., Hanson, C., Hatakka, J., He, Y., Hehn, M., Heinesch, B., Hinko-Najera, N., Hörtnagl, L., Hutley, L., Ibrom, A., Ikawa, H., Jackowicz-Korczynski, M., Janouš, D., Jans, W., Jassal, R., Jiang, S., Kato, T., Khomik, M., Klatt, J., Knohl, A., Knox, S., Kobayashi, H., Koerber, G., Kolle, O., Kosugi, Y., Kotani, A., Kowalski, A., Kruijt, B., Kurbatova, J., Kutsch, W.L., Kwon, H., Launiainen, S., Laurila, T., Law, B., Leuning, R., Li, Yingnian, Liddell, M., Limousin, J.-M., Lion, M., Liska, A.J., Lohila, A., López-Ballesteros, A., López-Blanco, E., Loubet, B., Loustau, D., Lucas-Moffat, A., Lüers, J., Ma, S., Macfarlane, C., Magliulo, V., Maier, R., Mammarella, I., Manca, G., Marcolla, B., Margolis, H.A., Marras, S., Massman, W., Mastepanov, M., Matamala, R., Matthes, J.H., Mazzenga, F., McCaughey, H., McHugh, I., McMillan, A.M.S., Merbold, L., Meyer, W., Meyers, T., Miller, S.D., Minerbi, S., Moderow, U., Monson, R.K., Montagnani, L., Moore, C.E., Moors, E., Moreaux, V., Moureaux, C., Munger, J.W., Nakai, T., Neirynck, J., Nesic, Z., Nicolini, G., Noormets, A., Northwood, M., Nosetto, M., Nouvellon, Y., Novick, K., Oechel, W., Olesen, J.E., Ourcival, J.-M., Papuga, S.A., Parmentier, F.-J., Paul-Limoges, E., Pavelka, M., Peichl, M., Pendall, E., Phillips, R.P., Pilegaard, K., Pirk, N., Posse, G., Powell, T., Prasse, H., Prober, S.M., Rambal, S., Rannik, Ü., Raz-Yaseef, N., Reed, D., de Dios, V.R., Restrepo-Coupe, N., Reverter, B.R., Roland, M., Sabbatini, S., Sachs, T., Saleska, S.R., Sánchez-Cañete, E.P., Sanchez-Mejia, Z.M., Schmid, H.P., Schmidt, M., Schneider, K., Schrader, F., Schroder, I., Scott, R.L., Sedlák, P., Serrano-Ortíz, P., Shao, C., Shi, P., Shironya, I., Siebicke, L., Šigut, L., Silberstein, R., Sirca, C., Spano, D., Steinbrecher, R., Stevens, R.M., Sturtevant, C., Suyker, A., Tagesson, T., Takanashi, S., Tang, Y., Tapper, N., Thom, J., Tiedemann, F., Tomassucci, M., Tuovinen, J.-P., Urbanski, S., Valentini, R., van der Molen, M., van Gorsel, E., van Huissteden, K., Varlagin, A., Verfaillie, J., Vesala, T., Vincke, C., Vitale, D., Vygodskaya, N., Walker, J.P., Walter-Shea, E., Wang, H., Weber, R., Westermann, S., Wille, C., Wofsy, S., Wohlfahrt, G., Wolf, S., Woodgate, W., Li, Yuelin, Zampedri, R., Zhang, J., Zhou, G., Zona, D., Agarwal, D., Biraud, S., Torn, M., Papale, D., 2020. The FLUXNET2015 dataset and the ONEFlux processing pipeline for eddy covariance data. Scientific Data 7, 225. https://doi.org/10.1038/s41597-020-0534-3

Peter, H., Singer, G.A., Preiler, C., Chifflard, P., Steniczka, G., Battin, T.J., 2014. Scales and drivers of temporal pCO_2 dynamics in an Alpine stream. Journal of Geophysical Research: Biogeosciences 119, 1078–1091. https://doi.org/10.1002/2013JG002552

Pighini, S., Ventura, M., Miglietta, F., Wohlfahrt, G., 2018. Dissolved greenhouse gas concentrations in 40 lakes in the Alpine area. Aquat Sci 80, 32. https://doi.org/10.1007/s00027-018-0583-2

Pirk, N., Sievers, J., Mertes, J., Parmentier, F.-J.W., Mastepanov, M., Christensen, T.R., 2017. Spatial variability of CO_2 uptake in polygonal tundra: assessing low-frequency disturbances in eddy covariance flux estimates. Biogeosciences 14, 3157–3169. https://doi.org/10.5194/bg-14-3157-2017

Podgrajsek, E., Sahlée, E., Rutgersson, A., 2015. Diel cycle of lake-air CO_2 flux from a shallow lake and the impact of waterside convection on the transfer velocity. J. Geophys. Res. Biogeosci. 120, 2014JG002781. https://doi.org/10.1002/2014JG002781

Polsenaere, P., Deborde, J., Detandt, G., Vidal, L.O., Pérez, M.A.P., Marieu, V., Abril, G., 2013. Thermal enhancement of gas transfer velocity of CO_2 in an Amazon floodplain lake revealed by eddy covariance measurements. Geophys. Res. Lett. 40, 1734–1740. https://doi.org/10.1002/grl.50291

Potes, M., Salgado, R., Costa, M.J., Morais, M., Bortoli, D., Kostadinov, I., Mammarella, I., 2017. Lake–atmosphere interactions at Alqueva reservoir: a case study in the summer of 2014. Tellus A: Dynamic Meteorology and Oceanography 69, 1272787. https://doi.org/10.1080/16000870.2016.1272787

Prairie, Y.T., Cole, J.J., 2009. Carbon, Unifying Currency, in: Likens, G.E. (Ed.), Encyclopedia of Inland Waters. Academic Press, Oxford, pp. 743–746. https://doi.org/10.1016/B978-012370626-3.00107-1

Pypker, T.G., Unsworth, M.H., Lamb, B., Allwine, E., Edburg, S., Sulzman, E., Mix, A.C., Bond, B.J., 2007. Cold air drainage in a forested valley: Investigating the feasibility of monitoring ecosystem metabolism. Agricultural and Forest Meteorology 145, 149–166. https://doi.org/10.1016/j.agrformet.2007.04.016

Raymond, P.A., Hartmann, J., Lauerwald, R., Sobek, S., McDonald, C., Hoover, M., Butman, D., Striegl, R., Mayorga, E., Humborg, C., Kortelainen, P., Dürr, H., Meybeck, M., Ciais, P., Guth, P., 2013. Global carbon dioxide emissions from inland waters. Nature 503, 355–359. https://doi.org/10.1038/nature12760

Read, J.S., Hamilton, D.P., Desai, A.R., Rose, K.C., MacIntyre, S., Lenters, J.D., Smyth, R.L., Hanson, P.C., Cole, J.J., Staehr, P.A., Rusak, J.A., Pierson, D.C., Brookes, J.D., Laas, A., Wu, C.H., 2012. Lake-size dependency of wind shear and convection as controls on gas exchange. Geophys. Res. Lett. 39, L09405. https://doi.org/10.1029/2012GL051886

Reed, D.E., Dugan, H.A., Flannery, A.L., Desai, A.R., 2018. Carbon sink and source dynamics of a eutrophic deep lake using multiple flux observations over multiple years. Limnology and Oceanography Letters 3, 285–292. https://doi.org/10.1002/lol2.10075

Shao, C., Chen, J., Stepien, C.A., Chu, H., Ouyang, Z., Bridgeman, T.B., Czajkowski, K.P., Becker, R.H., John, R., 2015. Diurnal to annual changes in latent, sensible heat, and CO_2 fluxes over a Laurentian Great Lake: A case study in Western Lake Erie. J. Geophys. Res. Biogeosci. 120, 2015JG003025. https://doi.org/10.1002/2015JG003025

Sievers, J., 2019. Ogive optimization toolbox (https://www.mathworks.com/matlabcentral/fileexchange/53545-ogive-optimization-toolbox). MATLAB Central File Exchange. Retrieved February 07, 2020.

Sievers, J., Papakyriakou, T., Larsen, S.E., Jammet, M.M., Rysgaard, S., Sejr, M.K., Sørensen, L.L., 2015a. Estimating surface fluxes using eddy covariance and numerical ogive optimization. Atmos. Chem. Phys. 15, 2081–2103. https://doi.org/10.5194/acp-15-2081-2015

Sievers, J., Sørensen, L.L., Papakyriakou, T., Else, B., Sejr, M.K., Haubjerg Søgaard, D., Barber, D., Rysgaard, S., 2015b. Winter observations of CO_2 exchange between sea ice and the atmosphere in a coastal fjord environment. The Cryosphere 9, 1701–1713. https://doi.org/10.5194/tc-9-1701-2015

Sollberger, S., Wehrli, B., Schubert, C.J., DelSontro, T., Eugster, W., 2017. Minor methane emissions from an Alpine hydropower reservoir based on monitoring of diel and seasonal variability. Environ. Sci.: Processes Impacts 19, 1278–1291. https://doi.org/10.1039/C7EM00232G

Spafford, L., Risk, D., 2018. Spatiotemporal Variability in Lake-Atmosphere Net CO_2 Exchange in the Littoral Zone of an Oligotrophic Lake. Journal of Geophysical Research: Biogeosciences 123, 1260–1276. https://doi.org/10.1002/2017JG004115

Sun, J., Desjardins, R., Mahrt, L., MacPherson, 1998. Transport of carbon dioxide, water vapor, and ozone by turbulence and local circulations. Journal of Geophysical Research: Atmospheres 103, 25873–25885. https://doi.org/10.1029/98JD02439

Tranvik, L.J., Downing, J.A., Cotner, J.B., Loiselle, S.A., Striegl, R.G., Ballatore, T.J., Dillon, P., Finlay, K., Fortino, K., Knoll, L.B., Kortelainen, P.L., Kutser, T., Larsen, Soren., Laurion, I., Leech, D.M., McCallister, S.L., McKnight, D.M., Melack, J.M., Overholt, E., Porter, J.A., Prairie, Y., Renwick, W.H., Roland, F., Sherman, B.S., Schindler, D.W., Sobek, S., Tremblay, A., Vanni, M.J., Verschoor, A.M., von Wachenfeldt, E., Weyhenmeyer, G.A., 2009. Lakes and reservoirs as regulators of carbon cycling and climate. Limnol. Oceanogr. 54, 2298–2314. https://doi.org/10.4319/lo.2009.54.6_part_2.2298

Vachon, D., Prairie, Y.T., 2013. The ecosystem size and shape dependence of gas transfer velocity versus wind speed relationships in lakes. Canadian Journal of Fisheries and Aquatic Sciences. https://doi.org/10.1139/cjfas-2013-0241

Vachon, D., Prairie, Y.T., Cole, J.J., 2010. The relationship between near-surface turbulence and gas transfer velocity in freshwater systems and its implications for floating chamber measurements of gas exchange. Limnology and Oceanography 55, 1723–1732. https://doi.org/10.4319/lo.2010.55.4.1723

Vesala, T., Huotari, J., Rannik, Ü., Suni, T., Smolander, S., Sogachev, A., Launiainen, S., Ojala, A., 2006. Eddy covariance measurements of carbon exchange and latent and sensible heat fluxes over a boreal lake for a full open-water period. Journal of Geophysical Research 111. https://doi.org/10.1029/2005JD006365

Vickers, D., Mahrt, L., 1997. Quality Control and Flux Sampling Problems for Tower and Aircraft Data. J. Atmos. Oceanic Technol. 14, 512–526. https://doi.org/10.1175/1520-0426(1997)014<0512:QCAFSP>2.0.CO;2

Vihma, T., Savijärvi, H., 1991. On the effective roughness length for heterogeneous terrain. Quarterly Journal of the Royal Meteorological Society 117, 399–407. https://doi.org/10.1002/qj.49711749808

Vingiani, F., Durighetto, N., Klaus, M., Schelker, J., Labasque, T., Botter, G., 2020. Evaluating stream CO_2 outgassing via Drifting and Anchored flux chambers in a controlled flume experiment. Biogeosciences Discussions 1–25. https://doi.org/10.5194/bg-2020-327

Wanninkhof, R., 1992. Relationship between wind speed and gas exchange over the ocean. Journal of Geophysical Research: Oceans 97, 7373–7382. https://doi.org/10.1029/92JC00188

Wanninkhof, R., Ledwell, J.R., Broecker, W.S., 1985. Gas Exchange-Wind Speed Relation Measured with Sulfur Hexafluoride on a Lake. Science 227, 1224–1226. https://doi.org/10.1126/science.227.4691.1224

Weiss, R.F., 1974. Carbon dioxide in water and seawater: the solubility of a non-ideal gas. Marine Chemistry 2, 203–215. https://doi.org/10.1016/0304-4203(74)90015-2

Zscheischler, J., Mahecha, M.D., Avitabile, V., Calle, L., Carvalhais, N., Ciais, P., Gans, F., Gruber, N., Hartmann, J., Herold, M., Ichii, K., Jung, M., Landschützer, P., Laruelle, G.G., Lauerwald, R., Papale, D., Peylin, P., Poulter, B., Ray, D., Regnier, P., Rödenbeck, C., Roman-Cuesta, R.M., Schwalm, C., Tramontana, G., Tyukavina, A., Valentini, R., van der Werf, G., West, T.O., Wolf, J.E., Reichstein, M., 2017. Reviews and syntheses: An empirical spatiotemporal description of the global surface–atmosphere carbon fluxes: opportunities and data limitations. Biogeosciences 14, 3685–3703. https://doi.org/10.5194/bg-14-3685-2017

Reference	Lake/Location	Lake Area (km^2)	Lake max. depth (m)	Lake mean depth (m)	Time frame
our study (Scholz et al. 2021)	Lake Lunz, Austria	0.68	34	20	1 year (2017)
Anderson et al., 1999	Williams Lake, MN, USA	0.37	9	5.2	5x1 week (spring/summer/fall)
Armani et al., 2020	Itaipu Lake, Brazil	1350			Jan - Nov 2013 (non-continuous)
Czikowsky et al., 2018	Lake Pleasant, NY, USA	6	24	8.0	16. Sept - 11. Oct 2010
Du et al., 2018	Erhai Lake, China	256.5	20.7	10.0	2012 - 2015
Erkkilä et al., 2018	Lake Kuivajärvi, Finnland	0.62	13.2	6.3	fall 2014 (16 days)
Eugster et al., 2003	Toolik Lake, Alaska	1.5	25		short term (2-4 days in July)
Eugster et al., 2003	Soppensee, Switzerland	0.25	27		short term (3 days in September)
Eugster et al., 2020	Toolik Lake, Alaska	1.5	26		ice free periods 2010-2015
Franz et al., 2016	Polder Zarnekow, Germany	0.075	1.2		May 2013 - May 2014
Han et al., 2020	Ngoring Lake, Tibet	610.7	32	17.0	ice free periods 2011-2013
Huotari et al., 2011, see also Vesala et al., 2006	Lake Valkea-Kotinen, Finland	0.041	6.5	2.5	ice free periods 2003-2007
Jammet et al., 2017	Villasjön, Sweden	0.17	1.3	0.7	Jun 2012 - Dec 2014
Jonsson et al., 2008	Lake Merasjärvi, Sweden	3.8	17	5.1	Jun - Okt 2005

Reference	Lake/Location	Lake Area (km^2)	Lake max. depth (m)	Lake mean depth (m)	Time frame
Kim et al., 2016	Eastmain-1 reservoir, Canada	603	57	11.0	ice free 2006-2009
Liu et al., 2015	Erhai Lake, China	256.5	20.7	10.0	1 yr (2012)
Liu et al., 2016	Ross Barnett Reservoir, MS, USA	134	8	4-8	1 yr (2008)
Lohila et al., 2015	Pallasjärv, Finland	17.3	36	9.0	Jul-Oct 2013
Mammarella et al., 2015, see also Heiskanen et al., 2014	Lake Kuivajärvi, Finland	0.63	13.2	6.4	Jun - Oct 2010 & 2011
Morin et al., 2017	Douglas Lake, MI, USA	13.74	24		Jun - Sept/Oct 2013 & 2014
Podgrajsek et al., 2015	Lake Tämnaren, Sweden	38	2	1.3	Sept 2010 - Sept 2012
Polsenaere et al., 2013	Floodplain lake, Barzil	450			19.-22.Nov 2011
Potes et al., 2017	Alqueva reservoir, Portugal	250	92	16.6	2. Jun-2. Oct 2014
Reed et al., 2018	Lake Mendota, WI, USA	39.61	25.3	12.8	2012-2017
Shao et al., 2015, see also Ouyang et al., 2017	Lake Erie, USA	25700	64	5.1	Oct 2011 - Sept 2013
Sollberger et al., 2017	Lake Klöntal, Switzerland	3.3	45		Mar - Jun 2012

Reference	Instrumentation: Open path (OP)/Close path (CP) gas analysator and measurement height (m)	Instrument set-up **	EC processing software
our study (Scholz et al. 2021)	CP 3.9 m	shore	EddyPro / matlab OgO Toolbox
Anderson et al., 1999	CP & OP 1.2 m	fix	
Armani et al., 2020	OP	fix	
Czikowsky et al., 2018	CP 2 m	float	
Du et al., 2018	OP 2.5 m	fix	EddyPro
Erkkilä et al., 2018	CP 1.8 m	float	EddyUH
Eugster et al., 2003	CP 1.5 m	float	
Eugster et al., 2003	OP 2.8 m	float	
Eugster et al., 2020	CP 1.3 - 1.6 m	float	eth-flux software
Franz et al., 2016	CP 2.6 m	shore	EddyPro
Han et al., 2020	OP 3 m	fix	EddyPro
Huotari et al., 2011, see also Vesala et al., 2006	CP 1.5 m	float	
Jammet et al., 2017	OP 2.5 m	shore	EddyPro
Jonsson et al., 2008	OP 1.6 -2.6 m	fix	EcoFlux 1.4

Reference	Instrumentation: Open path (OP)/Close path (CP) gas analysator and measurement height (m)	Instrument set-up **	EC processing software
Kim et al., 2016	OP 13 m	fix	
Liu et al., 2015	OP 3.5 m	fix	EddyPro
Liu et al., 2016	OP 4 m	fix	
Lohila et al., 2015	CP 2.5 m	shore	
Mammarella et al., 2015, see also Heiskanen et al., 2014	CP 1.7 m	float	EddyUH
Morin et al., 2017	OP ~2 m	fix	
Podgrajsek et al., 2015	OP 4.7 m	fix	
Polsenaere et al., 2013	OP 4.6 m	shore	EdiRe
Potes et al., 2017	OP 2 m	float	
Reed et al., 2018	OP 11.6 m	shore	TK3
Shao et al., 2015, see also Ouyang et al., 2017	OP 15 m	fix	EdiRe
Sollberger et al., 2017	OP 1.5 m	float	eth-flux software
		** fix: solid base but not on shore (e.g. fixed in sediment; island) float: floating platform shore: on shore of lake	various methods for time lag estimation and spectral corrections were applied

Reference	averaging interval (min) / detrending ***	coordinate rotation	Quality checks and criteria for rejection (SST: steady state test; ITT: integral turbulence test)
our study (Scholz et al. 2021)	variable (OgO)	coordinate rotation	OgO; positive momentum flux
Anderson et al., 1999	30 / digital recursive filter	coordinate rotation	spectral inspection
Armani et al., 2020	10 / LD	coordinate rotation	
Czikowsky et al., 2018	15	raft motion corrected; coordinate rotation	SST > 30 %; fluxes with high low-frequency contribution (ogive); calm & unstable periods (z/L<-0.55)
Du et al., 2018	30 / BA	coordinate rotation	SST & ITT (flag 0-1-2); flag = 2 is discarded
Erkkilä et al., 2018	30 / LD	coordinate rotation	SST > 100 %; skewness, kurtosis; standard deviation of CO2 > 3 ppm
Eugster et al., 2003	30 / LD	coordinate rotation	positive momentum flux; spectral inspection
Eugster et al., 2003	5 / LD	coordinate rotation	positive momentum flux; spectral inspection
Eugster et al., 2020	30	coordinate rotation	9-level flag system according to Foken (in Aubinet 2012); only flag = 9 was rejected
Franz et al., 2016	30 / BA	planar fit	flag 0-1-2; flag = 2 is discarded; u* < 0.12 or > 0.76 m s-1; flux <0.2 or >99.8 percentile
Han et al., 2020	30 / LD	coordinate rotation	
Huotari et al., 2011, see also Vesala et al., 2006	30 / LD	coordinate rotation	SST > 30 %; positive momentum flux; intermittency, skewness, kurtosis (Vickers & Mahrt 1997); vertical rotation > 15°
Jammet et al., 2017	30 / BA	coordinate rotation	SST > 30 %; skewness, kurtosis (Vickers & Mahrt 1997); when no time-lag found
Jonsson et al., 2008	30 / BA	coordinate rotation	SST > 30 %; positive momentum flux; CO2 fluxes outside 3 std

Reference	averaging interval (min) / detrending ***	coordinate rotation	Quality checks and criteria for rejection (SST: steady state test; ITT: integral turbulence test)
Kim et al., 2016	30 / BA	coordinate rotation	
Liu et al., 2015	30 / BA	coordinate rotation	Foken et al. 2004
Liu et al., 2016	30	coordinate rotation	Foken et al. 2004; negative CO2 fluxes outside 2-4 std were discarded
Lohila et al., 2015	30 / BA	coordinate rotation	SST; variance of CO2 concentration > 1 ppm
Mammarella et al., 2015, see also Heiskanen et al., 2014	30 / BA	coordinate rotation	skewness, kurtosis (Vickers & Mahrt 1997); SST > 100 %
Morin et al., 2017	30 / BA	coordinate rotation	u* threshold
Podgrajsek et al., 2015	30 / LD	coordinate rotation	u spd < 1 m s-1; skewness, kurtosis (Vickers & Mahrt 1997)
Polsenaere et al., 2013	10 / LD	coordinate rotation	SST & ITT
Potes et al., 2017	30 / LD	coordinate rotation	only diagnostic flags from instruments+wind direction/footprint
Reed et al., 2018	30	polynomal planar fit	default TK3 (SST & ITT)
Shao et al., 2015, see also Ouyang et al., 2017	30 / BA	planar fit	SST & ITT, u* < 0.1; flux > 6std (7day moving window)
Sollberger et al., 2017	30	NA	SST (Foken et al. 2012)
	*** BA: Block Average LD: Linear Detrending	most of the time, 'coordinate rotation' equals a double rotation.	

Reference	data cover (%)	Gap-filling	CO_2 flux ($mg\ C\ m^{-2}\ d^{-1}$)
our study (Scholz et al. 2021)	15%		259
Anderson et al., 1999			-186 to 2800
Armani et al., 2020			301
Czikowsky et al., 2018	35%		348
Du et al., 2018	55%	different methods for gap-filling were tested	322 to 443
Erkkilä et al., 2018	27%		363 to 1130
Eugster et al., 2003			114
Eugster et al., 2003			289
Eugster et al., 2020	51-93%	median diel cycle approach for short gaps up to 1.5 days; longer gaps: daily average of the respective season	200
Franz et al., 2016	45.5%	marginal distribution sampling	118
Han et al., 2020	80%		-830 to 130
Huotari et al., 2011, see also Vesala et al., 2006	10%		210 (186 to 266)
Jammet et al., 2017	26%	Artificial Neural Network	228
Jonsson et al., 2008	16%		221

Reference	data cover (%)	Gap-filling	CO_2 flux (mg C m^{-2} d^{-1})
Kim et al., 2016			1140
Liu et al., 2015			466 to 1284
Liu et al., 2016	80%		321
Lohila et al., 2015			210
Mammarella et al., 2015, see also Heiskanen et al., 2014	37%		726
Morin et al., 2017	51-73 %	Neural Network (separately for night-time and daytime data)	726
Podgrajsek et al., 2015	45%		187
Polsenaere et al., 2013	62%		612
Potes et al., 2017	63%		-38
Reed et al., 2018	29 % (?)		-151 to -636
Shao et al., 2015, see also Ouyang et al., 2017	35%	marginal distribution sampling (monthly mean / MDV were also tested)	173
Sollberger et al., 2017	83.7 % (26.4 % best QC)		15.5

JGR Biogeosciences

Supporting Information for

Atmospheric CO_2 exchange of a small mountain lake: limitations of eddy covariance and boundary layer modeling methods in complex terrain.

Katharina Scholz[1*], Elisabet Ejarque[2], Albin Hammerle[1], Martin Kainz[2], Jakob Schelker[2,3], Georg Wohlfahrt[1]

1) Department of Ecology, University of Innsbruck, Sternwartestrasse 15, 6020 Innsbruck, Austria.

2) WasserCluster Lunz – Biologische Station, Dr. Carl Kupelwieser Promenade 5, 3293 Lunz am See, Austria.

3) Department of Functional and Evolutionary Ecology, University of Vienna, Althanstrasse 14, 1090 Vienna, Austria.

Contents of this file

Additional Supporting Information (Files uploaded separately)

Introduction

Because the ogive optimization (OgO) method is not commonly applied in eddy covariance (EC) data processing, a short summary of the method and its background as developed and described by Sievers et al. (2015 a) is given in the following. In addition, the application of the OgO method at our field site – a small mountain lake – is exemplified and discrepancies between the estimated fluxes resulting from the OgO method and the conventional EC data processing are presented.

Text S1 – Additional information on the ogive optimization method.

The OgO is an alternative approach to process EC data to estimate turbulent exchange while separating out low-frequency contributions (Sievers et al., 2015).

An ogive is an empirical cumulative distribution and here refers to the cumulative integral of the co-spectra of CO_2 concentration and vertical wind speed (w) from high to low frequencies, where the co-spectrum is the spectral decomposition of the flux estimate. Therefore, an ogive represents the cumulative contribution of different frequencies to the calculated flux. In theory, the ogive converges towards an asymptote with decreasing frequencies within an optimum averaging interval (Figure S1 a). However, the inclusion of low frequency contributions may lead to a continuous increase (Figure S1 b) or reversal (Figure S1 c) of the ogive curve depending on the direction of the low frequency motions. Low frequency contribution can be minimized by choosing the ideal averaging interval. Also, pre-treatment of the data with an appropriate detrending method can help to reduce non-turbulent influence. However, in cases where the frequency range of turbulence and low-frequency contributions overlaps, the estimation of the ideal averaging time or detrending method is not straightforward.

The OgO method generates an ogive density map by calculating ogives for a multiplicity of data permutations based on different combinations of averaging times and detrending methods for a certain time window at any chosen point in time (Figure S1, grey shades). Subsequently, a spectral distribution model is fitted to the obtained density map and the best fit (Figure S1, blue lines) is assumed to represent the pure turbulent flux.

In our study, the EC method was used to quantify lake-atmosphere CO_2 exchange. Fluxes calculated using the standard EC processing (using EddyPro 6.2.1, LI-COR Inc., Lincoln, NE, USA) showed large short-term temporal variation and the spectral analysis of the raw data indicated high low-frequency contributions. Therefore, the OgO method was applied to calculate CO_2 fluxes ($F_{c\text{-}Og}$) at this small mountain lake and the results were compared to the flux results of the standard EC processing ($F_{c\text{-}EC}$). In addition, the prevailing environmental conditions in relation to the differences between the results of the two processing methods were analyzed. To that end, a regression ensemble was trained to predict the differential CO_2 flux between the two processing methods based on air temperature (T_a), the surface water temperature estimated from outgoing longwave radiation (T_s), relative humidity (RH), net solar radiation (R_n), wind speed (u), friction velocity (u*), atmospheric stability (zoL), and wind direction at the opposing shore ($udir_W$) and the predictor importance and the related partial dependence were investigated. All analyzes were done in Matlab version R2019b (The MathWorks Inc., Natick, MA, USA).

In Figure S1, three examples for OgO flux estimations at Lake Lunz are shown. In all three panels, the red line marks the ogive as calculated for a 30min averaging interval with data linearly detrended, i.e., the conventional EC processing. The grey shades show the ogive density map based on the respective data permutations while the resulting modeled ogive is represented by the blue line. Panel a) shows a case where the conventionally calculated ogive (red line) closely follows the expected shape converging towards a constant value (about 0.4 µmol m^{-2} s^{-1} in that case) at the low frequency range (left end of the x axis). Therefore, the difference between F_{c-EC} and F_{c-Og} is small. However, at Lake Lunz, cases as depicted in panel b) and c) were more common, with variable low-frequency contributions often causing an unexpected increase or reversal of the ogive curve.

Overall, fluxes calculated using the OgO method showed less scatter than the conventional processing (Figure S2) and also a better agreement with the seasonal course of dissolved CO_2 and CO_2 flux estimates based on the BLM method, F_{c-BLM} (Figure S3).

The best predictors for differences in the fluxes calculated with the two processing methods (F_{c-EC} and F_{c-Og}) were wind speed and the wind direction at the opposing shore (which is an indicator of the persisting wind regime) (Figure S4 upper panel). In general, low wind speed and lake-breeze conditions led to the largest discrepancies between the two flux estimates (Figure S4 lower panels).

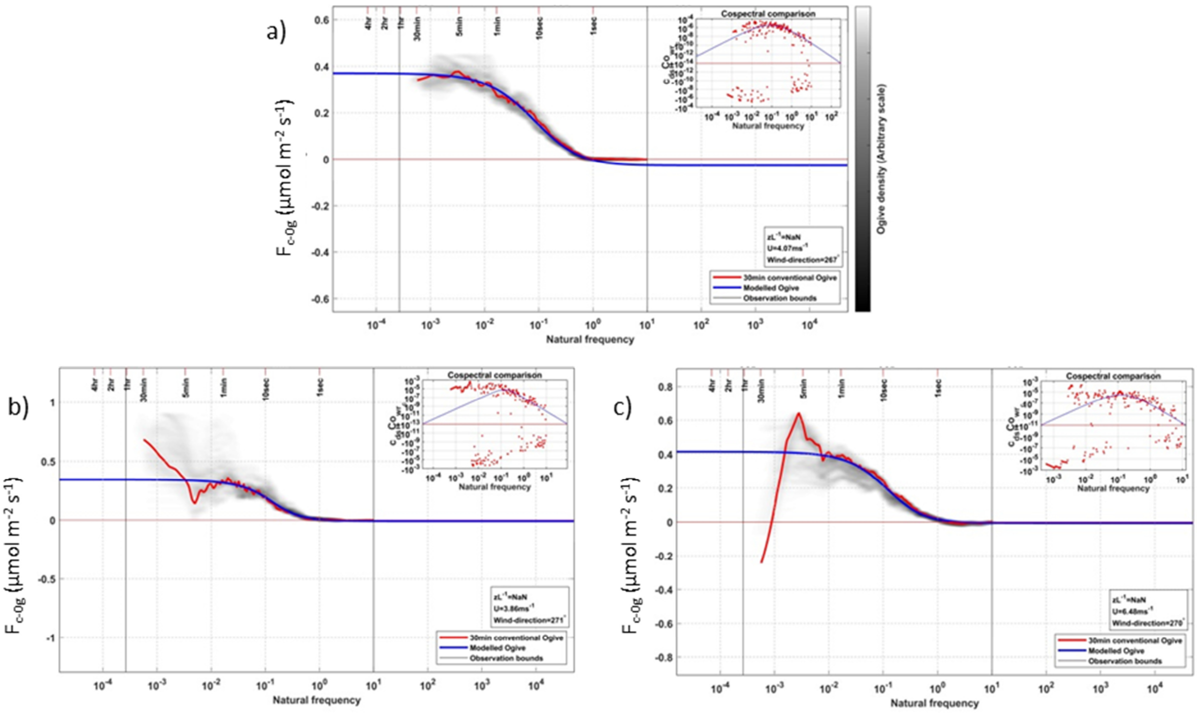

Figure S1. Three exemplary cases for flux estimates using the OgO method. The red line shows the standard 30min linear detrending. The grey shades denote the ogive density pattern of ogives calculated following data permutations. The best fit modeled ogive is shown in blue. The small inserted figures show equivalent co-spectra. Three situations are shown, where a) the standard ogive closely follows the expected shape and discrepancies between standard and modeled ogive are small, b) low-frequency contributions lead to a continuous increase of the ogive curve and therefore to flux overestimation, and c) low-frequency contributions cause a sign reversal and therefore to flux underestimation.

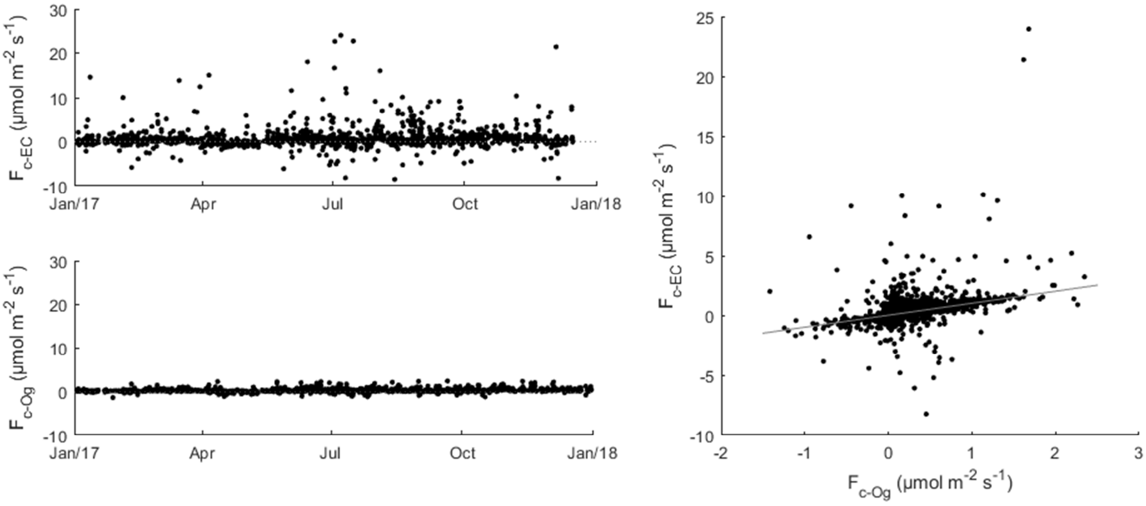

Figure S2. CO_2 flux estimates based on the standard EC processing ($F_{c\text{-}EC}$, top left), based on the OgO method ($F_{c\text{-}Og}$, bottom left), and a scatter plot of $F_{c\text{-}EC}$ and $F_{c\text{-}Og}$. The grey line in the scatter plot denotes the 1:1-line.

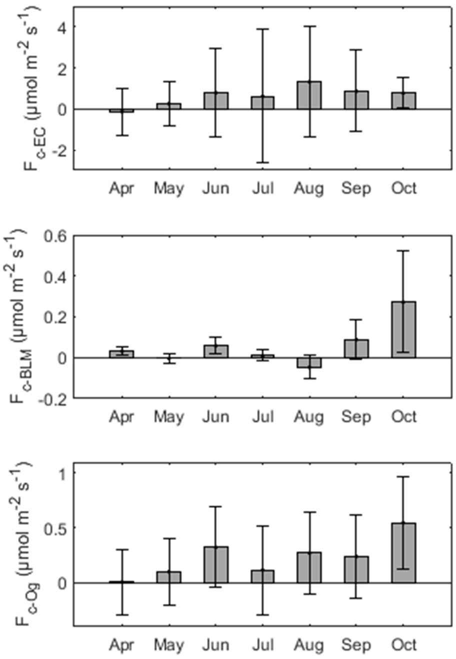

Figure S3. Monthly mean CO_2 fluxes estimated based on the standard EC (top), the BLM (middle), and the OgO (bottom) approach. Error bars show ± 1 standard deviation.

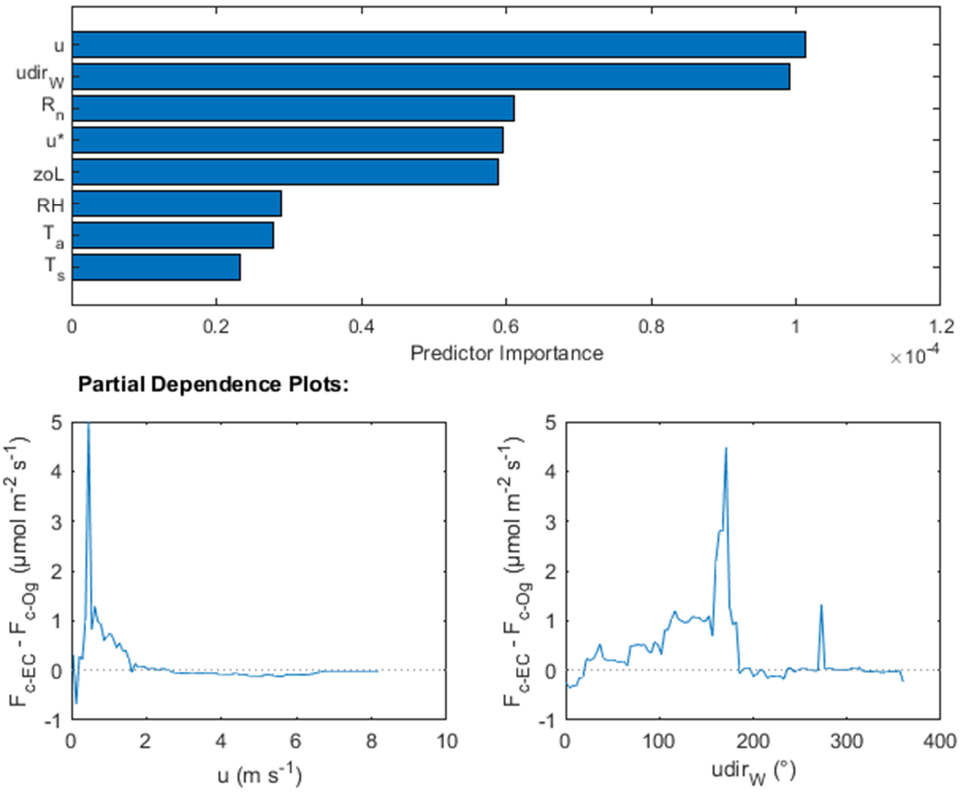

Figure S4. Predictor importance (top panel) of the trained regression ensemble. The partial dependence of the two most important predictors, wind speed u and wind direction at the opposing shore udir$_W$, is plotted in the lower panels.

Table S1. Overview of EC CO_2 flux measurements at lakes – additional information.